ELECTRONIC SUPPORTING INFORMATION

Exceptional TcO_4^- sorption capacity and highly efficient ReO_4^- luminescence sensing by Zr^{4+} MOFs

Sofia Rapti,[a]† Stavros A. Diamantis,[b]†Argyro Dafnomili,[b]†Anastasia Pournara,[a] Euaggelia Skliri,[c] Gerasimos S. Armatas,[c] Athanassios C. Tsipis,[a]Ioannis Spanopoulos,[d] Christos D. Malliakas.[d] Mercouri G. Kanatzidis,[d] John C. Plakatouras,[*,a] Fotini Noli,[*,b] Theodore Lazarides[*,b] and Manolis J. Manos[*,a]

[a.] *Department of Chemistry, University of Ioannina, 45110 Ioannina, Greece; email: iplakatu@cc.uoi.gr, email: iplakatu@cc.uoi.gr, emanos@cc.uoi.gr*

[b.] *Department of Chemistry, Aristotle University of Thessaloniki, 54124 Thessaloniki, Greece; email: noli@chem.auth.gr, tlazarides@chem.auth.gr*

[c.] *Department of Materials Science and Technology, University of Crete 71003 Heraklion, Greece.*

[d.] *Department of Chemistry, Northwestern University, Evanston, IL 60208*

† These authors contributed equally.

EXPERIMENTAL SECTION

Materials. All chemicals were purchased from Aldrich. The solvents were used as received. The water used was purified through a Millipore system.

SYNTHESES

MOR-1 and **MOR-2/MOR-2-HA** materials were prepared as reported in references 18 and 19 respectively (see main article).

ANALYTICAL AND CHARACTERIZATION TECHNIQUES

In house X-ray powder diffraction. Powder X-ray diffraction of the samples were measured at room temperature on a STOE-STADIMP powder diffractometer equipped with an asymmetric curved Germanium monochromator (CuKα1 radiation, λ = 1.54056 Å) and one-dimensional silicon strip detector (MYTHEN2 1K from DECTRIS). The line focused Cu X-ray tube was operated at 40 kV and 40 mA. Powder of each sample was packed in a 1 mm diameter polyimide capillary (polymer substrate with neither Bragg reflections nor broad peaks above 10 degrees) and measured in Debye-Scherrer geometry on a spinning stage (~ 200 rpm). Intensity data from 3 to 125 degrees two theta were collected over a period of 17 h with a step of 0.005 degrees. Instrument was calibrated against a NIST Silicon standard (640d) prior the measurement.

IR spectroscopy. IR spectra were recorded on KBr pellets in the 4000-400 cm^{-1} range using a Perkin-Elmer Spectrum GX spectrometer.

Energy dispersive spectroscopy (EDS) analyses. These measurements were performed on a JEOL (JEOL 6510 LV) scanning electron microscope (SEM) equipped with an Oxford dispersive X-ray spectroscopy (EDS) detector. Data acquisition was performed with an accelerating voltage of 20 kV and 120 s accumulation time.

Gas sorption measurements. N_2 adsorption-desorption isotherms were measured at 77 K on a Quantachrome Nova 3200*e* sorption analyzer. Before analysis, all samples were EtOH-exchanged, activated via supercritical CO_2 drying and then, degassed at 120 ºC under vacuum ($<10^{-5}$ Torr) for 12 h. The specific surface areas were calculated by applying the Brumauer-Emmett-Teller (BET) method to the branch of isotherms in the 0.05–0.25 relative pressure (P/P_o) range.

Re analyses by UV/Vis. The method for analysis of ReO_4^- via UV-Vis spectroscopy is described in reference: L. V. Borisova, A. N. Ermakov and A. B. lsmagulova, *Analyst* **1982,** *107***,** 495.

Inductively Coupled Plasma-Mass Spectroscopy (ICP-MS). Quantification of rhenium (Re) was accomplished using ICP-MS of acidified samples. Specifically, 300 µL of concentrated nitric acid (67-70% TraceMetal™ Grade, Fisher) was added to 50 µL aqueous samples. Ultra pure H_2O (18.2 MΩ·cm) is then added to produce a final sample solution of 10 mL. Quantitative standards were made using a commercial 1000 ppm Re solution (Sigma-Aldrich) which created a 100 ppb elemental standard. All samples (including standards and blank solution) contained 3% HNO_3 (67-70% TraceMetal™ Grade, Fisher).

ICP-MS was performed on a computer-controlled (QTEGRA software) Thermo iCapQ ICP-MS (Thermo Fisher Scientific, Waltham, MA, USA) operating in KED mode and equipped with an ESI SC-2DX PrepFAST autosampler (Omaha, NE, USA). Internal standard was added inline using the prepFAST system and consisted of 1 ng/mL of a mixed element solution containing Bi, In, ^{6}Li, Sc, Tb, Y (IV-ICPMS-71D from Inorganic Ventures). Online dilution was also carried out by the prepFAST system and used to generate calibration curves consisting of 1, 2, 5, 10, 20, 50, 100 ppb Re. Each sample was acquired using 1 survey run (10 sweeps) and 3 main (peak jumping) runs (40 sweeps). The isotopes selected for analysis were ^{185}Re and ^{187}Re. ^{89}Y and ^{159}Tb were also analyzed and were chosen as internal standards for data interpolation and machine stability. Instrument performance is optimized daily through autotuning followed by verification via a performance report (passing manufacturer specifications).

ION EXCHANGE STUDIES

Preparation of the column. 50 mg of **MOR-2-HA** composite and 5 g of sand (50-70 mesh SiO_2) was mixed in a mortar and pestle and filled in a glass column (0.7 cm ID column). Prior the ion exchange studies, the column was washed with ~ 7 mL HCl (4 M) solution and deionized water.

Batch ReO_4^- ion-exchange studies. A typical ion-exchange experiment of **MOR-1** or **MOR-2** with ReO_4^- is the following: In a solution of $NaReO_4$ (0.4 mmol) in water (10 mL, pH ~ 7), compound **MOR-1** or **2**(~ 0.04 mmol) was added as a solid. The mixture was kept under

magnetic stirring for ~ 20 min. Then, the polycrystalline material was isolated by filtration, washed several times with water and acetone and dried in the air.

The ReO_4^- uptake from solutions of various concentrations (0.6-15 mM) was studied by the batch method at *V*:*m* ~ 1000 mL/g, room temperature and 1 h contact. Re analysis has been made via UV-Vis (for Re concentrations up to 4-5 ppm) or ICP-MS (for lower Re concentrations). These data were used for the determination of ReO_4^- sorption isotherms. The competitive ion exchange experiments were also carried out with the batch method at *V*: *m* ratio ~ 1000 mL/g, room temperature and 1 h contact. For the determination of the sorption kinetics, ReO_4^- ion-exchange experiments of various reaction times (1-60 min) have been performed. For each experiment, a 10 mL sample of ReO_4^- solution was added to each vial (containing 10 mg of **MOR-1**, **MOR-2, UiO-66**) and the mixtures were kept under magnetic stirring for the designated reaction times. The suspensions from the various reactions were filtrated and the resulting solutions were analyzed for their chromium content with UV-Vis or ICP-MS. It should be also noted that UiO-66 was pretreated with 4 M HCl acid prior its use for ReO_4^- sorption studies.

Batch $^{99m}TcO_4^-$ ion-exchange studies.

For the Tc-sorption experiments perrhenate were used as chemical analog of pertechnetate. The tests were performed using NH_4ReO_4 solutions with $^{99m}TcO_4^-$ ($t_{1/2}$ of ^{99m}Tc 6.0 hours, I_Γ 141 keV) as tracer in the concentration region 10-5000 mg/L (0.054-26.9 mmol/L) (pH 2, dosage 15 mg of sorbent in 10 mL solution). $^{99m}TcO_4^-$ was eluted by 0.9% NaCl from a ^{99m}TcO generator and measured using gamma-spectroscopy with an HPGe detector (CANBERRA, efficiency 20%, energy resolution 2.1 keV for the 1332 keV of ^{60}Co γ-radiation).

Column Ion-Exchange studies

Several bed volumes of the solution were passed through the column and collected at the bottom in glass vials. The solutions were analyzed with UV-Vis or ICP-MS (for concentrations of Re < 3 ppm). The regeneration of the column was performed by its treatment with ~ 7 mL of HCl acid (4 M) solution. Then, the column is washed with enough water to remove excess acid. Column containing only sand as stationary phase showed no ReO_4^- sorption capacity.

FLUORESCENCE SENSING STUDIES

The fluorescence spectra were measured on a Hitachi F7000 spectrofluorometer. The light source was a Xenon arch lamp and the detector a red sensitive Hamamatsu R928 photomultiplyer tube. All spectra are corrected for instrument response using the correction function generated after calibration of the instrument with a standard light source. Appropriate long pass filters were used to remove scattering from the sample and the monochromators. For the Re(VII) sensing experiments, 1 mg of the MOF in the form of a fine powder were suspended in 10 mL of the respective medium (doubly distilled water or potable water) the pH of which was previously adjusted to 5 by careful addition of 4M HCl. The system was sonicated for 30 min and 1 mL of the resulting fine suspension was transferred to a luminescence quartz cuvette. Aliquots of NH_4ReO_4 10^{-3} M (dissolved in the same medium as the MOF) were added using a Hamilton™ precision microsyringe (50 μL range) in order to achieve the desired Re(VII) concentration. Emission spectra were recorded 2 min after each addition. The emission spectrum after each addition was recorded three times to ensure signal stability.

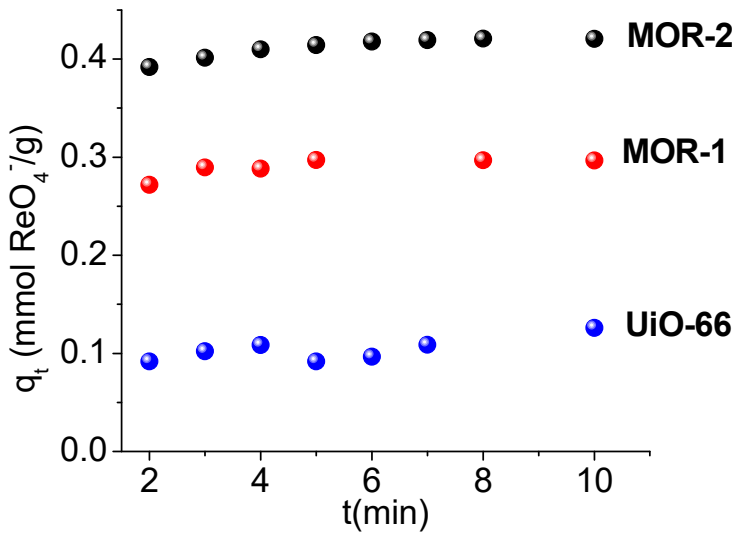

Figure S1. ReO_4^- sorption kinetics data for **MOR-1**, **MOR-2** and **UiO-66** materials (initial ReO_4^- concentration = 0.58 mM, pH ~7).

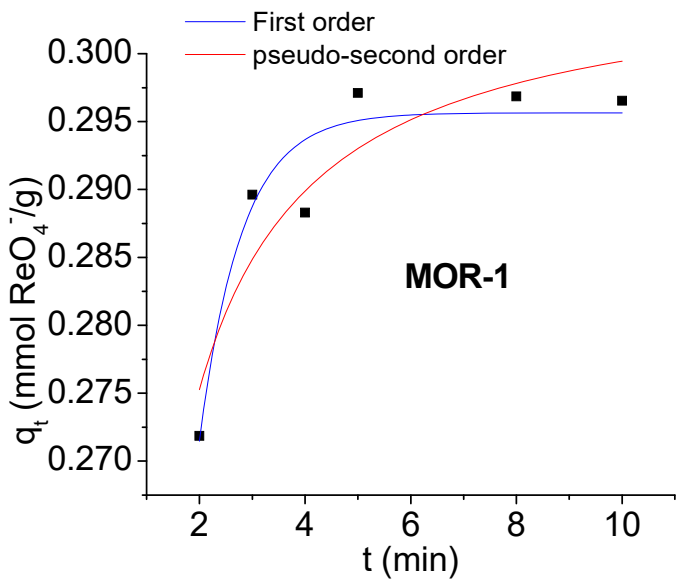

Figure S2. Fitting of the ReO_4^- sorption kinetics data for **MOR-1** with the Lagergren's First-order equation $\boldsymbol{q_t = q_e[1 - \exp(-K_L t)]}$

(Fitting data: R^2=0.90, q_e=0.296±0.001 mmol/g, K_L=1.25±0.07 min^{-1})

and the Ho and Mckay's pseudo-second-order equation

$$\boldsymbol{q_t = \frac{k_2 q_e t^2}{1 + k_2 q_e t}}$$

(Fitting data: R^2=0.83, q_e=0.306±0.004 mmol/g, k_2=14.5±3.3 g/mmol·min)

where q_t = the amount (mg/g) of ion sorbed by the sorbent at different reaction times (t), q_e= the amount (mg/g) of ion sorbed in equilibrium, K_L (min^{-1})= the Lagergren or first-order rate constant, k_2 (g/mmol·min)= the second-order rate constant.

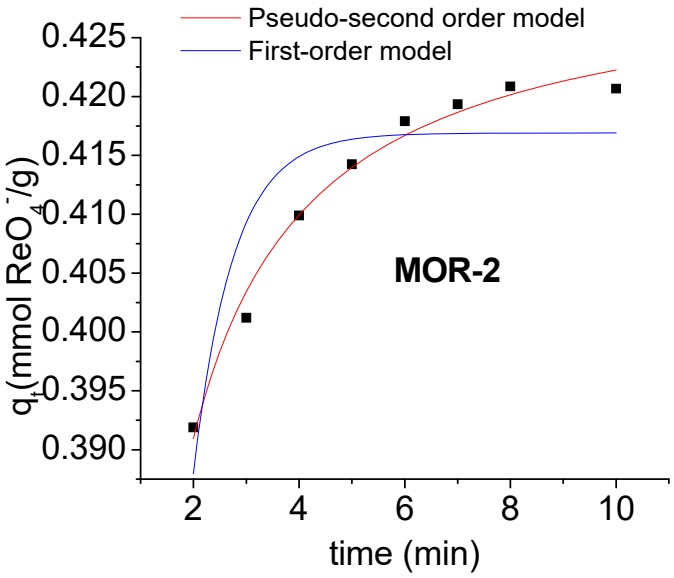

Figure S3. Fitting of the ReO_4^- sorption kinetics data for **MOR-2** with the Lagergren's First-order equation **(Fitting data: R^2=0.78, q_e=0.417±0.002 mmol/g, K_L=1.34±0.09 min^{-1})** and the Ho and Mckay's pseudo-second-order equation **(Fitting data: R^2=0.98, q_e=0.431±0.001 mmol/g, k_2=11.4±0.6 g/mmol·min).**

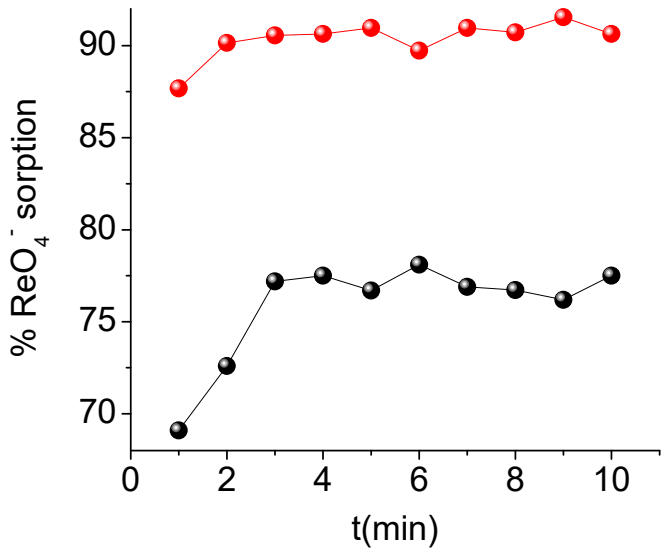

Figure S4. ReO_4^- sorption kinetics data for **MOR-2** with solutions of low initial ReO_4^- concentrations. Red and black spheres correspond to sorption data with initial ReO_4^- concentrations of 26.8 and 5.4 μM respectively. The lines are only a guide to the eye.

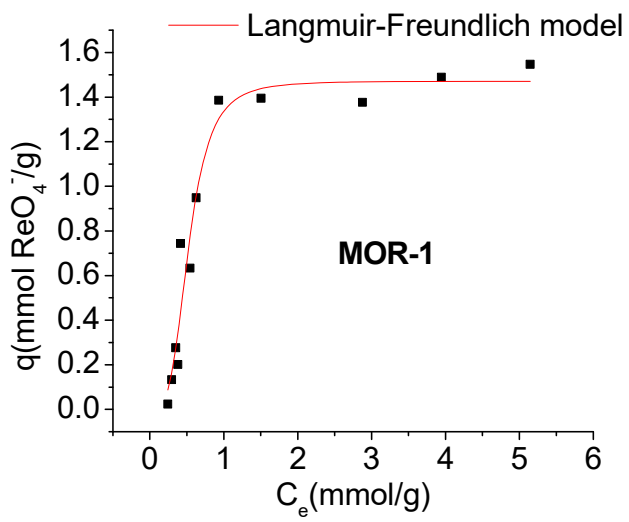

Figure S5. ReO_4^- sorption isotherm data for **MOR-1 (pH ~7)** and their fitting with the Langmuir-Freundlich model

$$q = q_m \frac{(bC_e)^{\frac{1}{n}}}{1+(bC_e)^{\frac{1}{n}}}$$

(Fitting data: R^2=0.95, q_m =1.47±0.07 mmol/g, b = 1.9±0.1 L/mmol, n = 0.28±0.06)

where q (mg/g) is the amount of the ion sorbed at the equilibrium concentration C_e (mmol/g), q_m (mmol/g) is the maximum sorption capacity of the sorbent, b (L/mmol) is the Langmuir constant, $1/n$ is a Freundlich constant. Fitting of the data with the Langmuir model

$$q = q_m \frac{bC_e}{1+bC_e}$$

is not satisfactory (R^2=0.79).

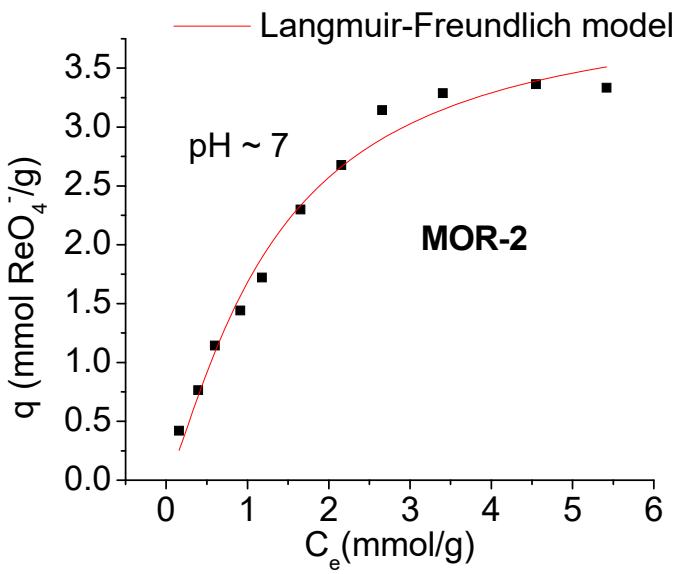

Figure S6. ReO_4^- sorption isotherm data for **MOR-2 (pH ~7)** and their fitting with the Langmuir-Freundlich model (**Fitting data: R^2=0.98, q_m =4.1±0.4 mmol/g, b = 0.75±0.13 L/mmol, n = 0.78±0.11)**. Fitting of the data can be also done with the Langmuir (**Fitting data: R^2=0.97, q_m =4.8±0.3 mmol/g, b = 0.54±0.08 L/mmol**) and Freundlich models (**Fitting data: R^2=0.93, K_F =1.65±0.12, n = 2±0.2**)

Freundlich equation:

$$q = K_F C_e^{\frac{1}{n}}$$

where K_F and $1/n$ are the Freundlich constants

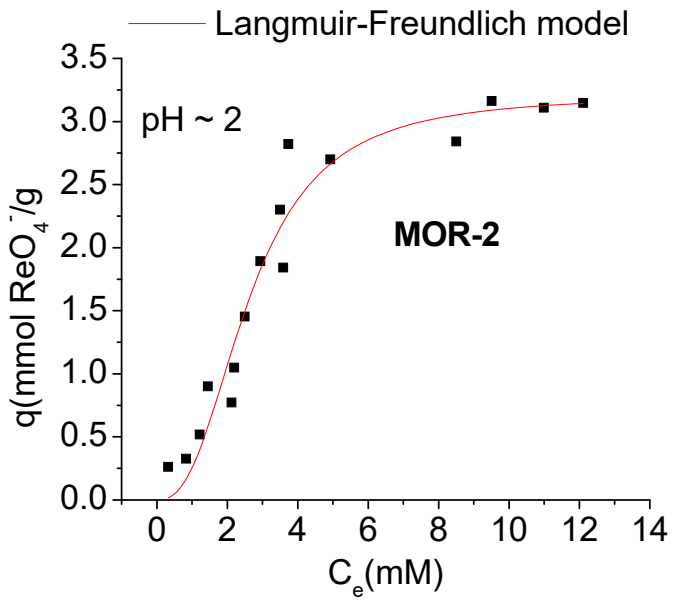

Figure S7. ReO_4^- sorption isotherm data for **MOR-2 (pH ~2)** and their fitting with the Langmuir-Freundlich model (**Fitting data: R^2=0.94, q_m =3.2±0.2 mmol/g, b = 0.38±0.03 L/mmol, n = 0.40±0.07).** Fitting of the data can be done also with the Langmuir (**Fitting data: R^2=0.88**, **q_m =4.9±0.7 mmol/g, b = 0.18±0.05 L/mmol**) and Freundlich models (**Fitting data: R^2=0.89**, **K_F =0.89±0.14, n = 1.8±0.3**), although the fitting with the Langmuir-Freundlich model is more satisfactory.

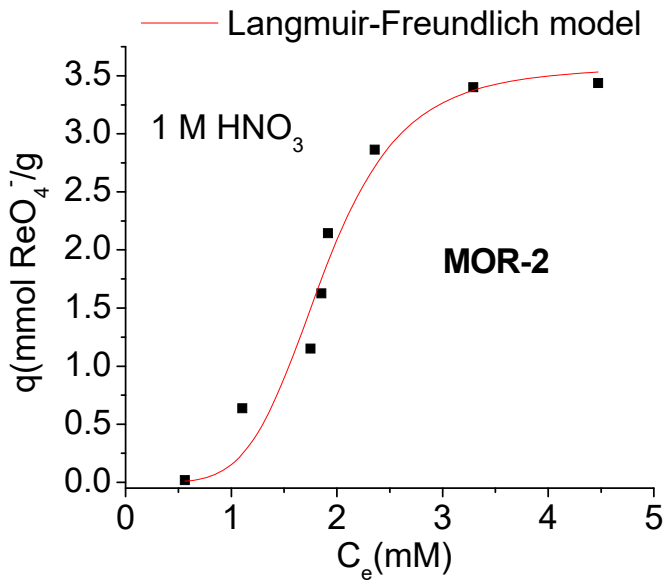

Figure S8. ReO_4^- sorption isotherm data for **MOR-2 (1 M HNO_3)** and their fitting with the Langmuir-Freundlich model (**Fitting data: R^2=0.95, q_m =3.6±0.3 mmol/g, *b* = 0.54±0.03 L/mmol, *n* = 0.20±0.06).** Fitting of the data with the Langmuir (R^2 =0.83) and Freundlich models (R^2 =0.82) was not satisfactory.

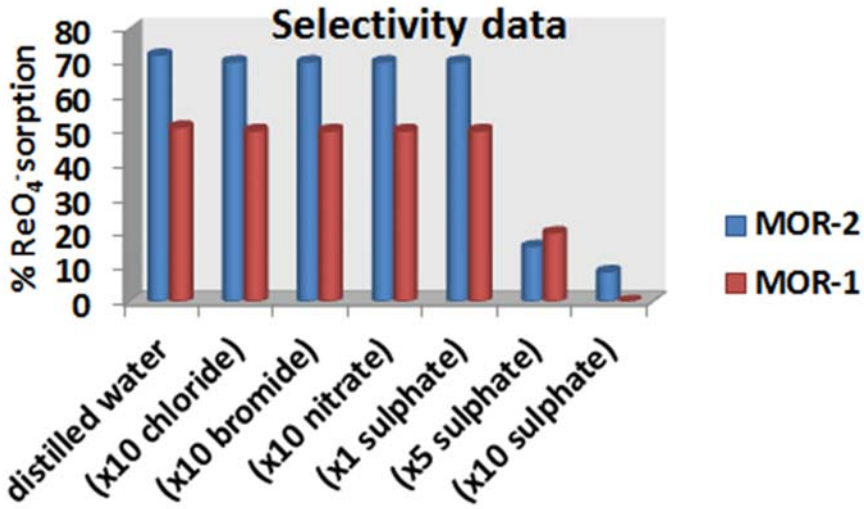

Figure S9. Results for the selectivity of **MOR-1** and **MOR-2** for the sorption of ReO_4^- vs. Cl^-, Br^-, NO_3^- and SO_4^{2-}.

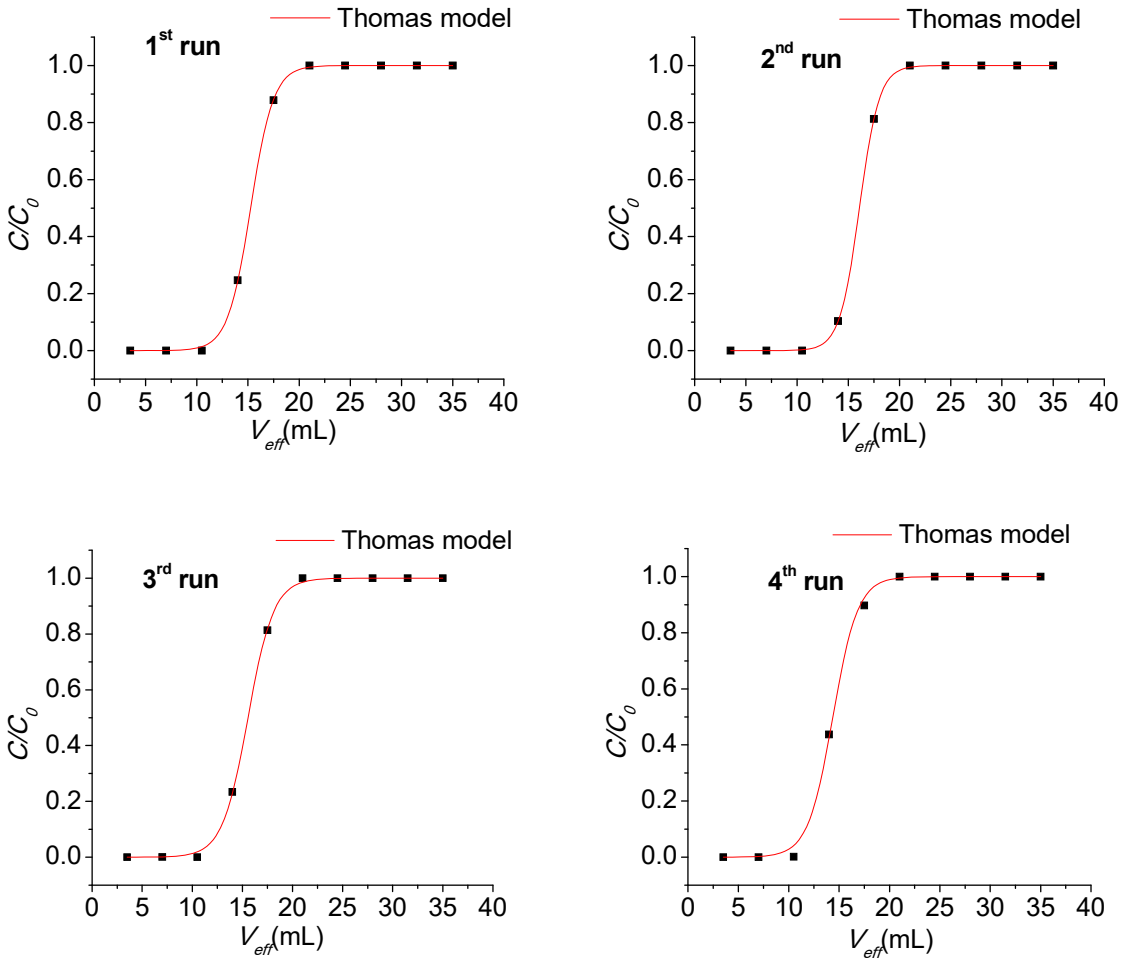

Figure S10. Fitting of the breakthrough curves (red line) for the column soprtion experiments of **MOR-2-HA** with the ReO_4^- solution (initial ReO_4^- concentration = 1.14 mM, pH~ 7, flow rate ~ 1.75 mL/min). The data are fitted with an equation (Thomas model) of the type $y = \frac{1}{1+\exp(A-Bx)}$, where A $= \frac{k_{Th} q_{\max} m}{Q}$, B$= \frac{k_{Th} C_0}{Q}$ (where C and C_0 represent the concentration (mmol L^{-1}) of the ion in the effluent and its initial concentration (mmol L^{-1}) respectively, k_{Th} (L $mmol^{-1}$ min^{-1}) is the Thomas model or sorption rate constant, q_{max} (mmol

g^{-1}) is the sorption capacity at the saturation point, m (mg) is the sorbent mass, Q and V_{eff} are the volumetric flow (mL min^{-1}) and the effluent volume (mL) respectively.

The results of the fitting are shown in Table S1.

Table S1. Fitting of the column sorption data and the experimentally found q_{max} values.

Run	Fitting results			Thomas model parameters	
	A	B	R^2	k_{Th} (L $mmol^{-1}$ min^{-1})	q_{max}($mmol^{-1}$ g^{-1})
1	13.667	0.896	0.999	1.374809	0.347946
2	16.728	1.040	0.999	1.596399	0.36674
3	12.107	0.778	0.999	1.194268	0.354816
4	11.606	0.807	0.999	1.238601	0.327951

The breakthrough capacity Q_b (mmol) can be determined by the equation:

$$\boldsymbol{Q_b = C_0 V_b}$$

where C_0 and V_b represent the initial concentration of ReO_4^- (mmol L^{-1}) and the volume (L) of the solution coming through the column until the breakpoint concentration (where the ReO_4^- is detected) respectively. For all runs ~ 100% removal of ReO_4^- was observed for 3 bed volumes or 10.5 ml of effluent. Thus, V_b= 10.5x10^{-3} L. Therefore, Q_b= 0.01197 mmol or ~0.24 mmol ReO_4^- /g (considering that the column contains 0.05 g of **MOR-2-HA**).

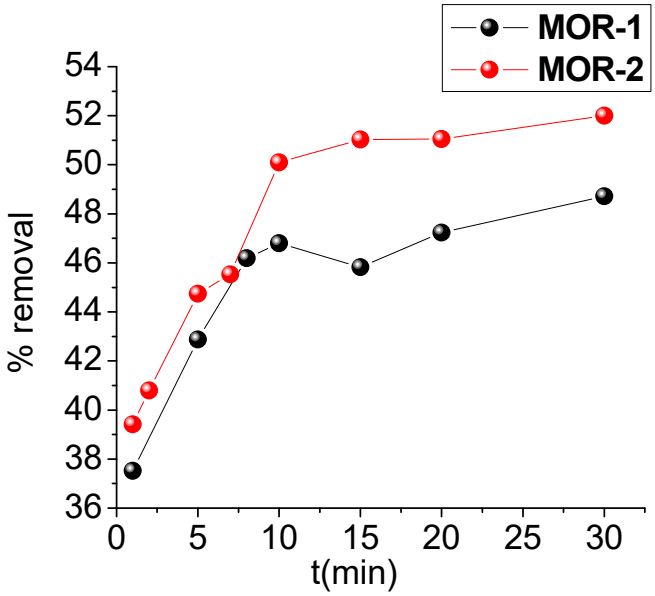

Figure S11. Kinetic sorption data that were determined using ReO_4^- solutions (0.54 mM, pH ~2) with $^{99m}TcO_4^-$ as tracer. The lines are only a guide to the eye.

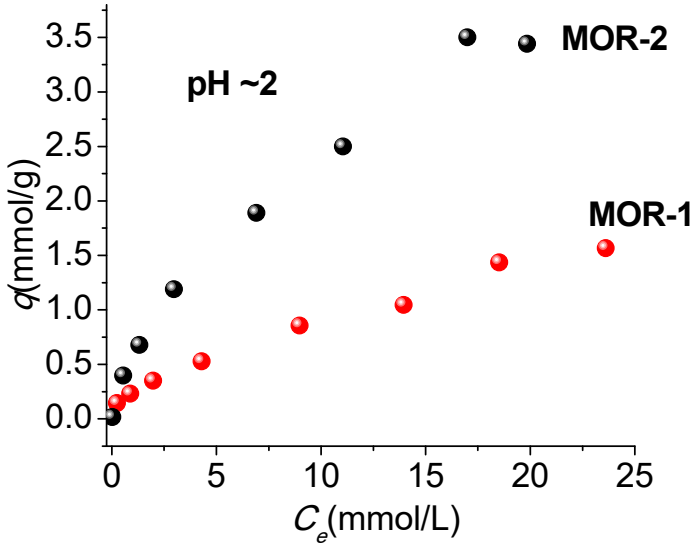

Figure S12. Isotherm sorption data that were determined using ReO_4^- solutions (0.054-26.9 mM, pH ~2) with $^{99m}TcO_4^-$ as tracer.

Computational Details

All calculations were performed using the Gaussian09 program suite.[1] The geometries of all stationary points were fully optimized, without symmetry constraints, employing the wB97XD functional from Head-Gordon and coworkers, which includes empirical dispersion.[2] For the geometry optimizations, we used the all electron ADZP basis set for Tc[3] and Re[4] metal atoms (M) which an augmented Gaussian basis set of double zeta valence quality while for the rest, non metal atoms (E) we used the 6-31+G(d) basis set. Hereafter, the computational protocol employed would be abbreviated as wB97XD/ADZP(M)U6-31+G(d)(E). All stationary points were identified as minima (number of imaginary frequencies Nimag = 0). Water solvent effects were taken into account with the polarizable continuum model (PCM) using the integral equation formalism variant (IEFPCM) being the default self-consistent reaction field (SCRF) method.[5] The binding energies, *BE*, corresponding to the interactions of the MO_4^- (M = Tc or Re) with the $[PhNH_3]^+$ and $[PhNH_2CH_2PyH]^{2+}$ ligands, were calculated according to the following equation:

$$BE = (E_{tot}[A]^+ + E_{tot}[MO_4]^-) - E_{tot}[A]^+[MO_4]^-$$

where $E_{tot}[A]^+$, $E_{tot}[MO_4]^-$ and $E_{tot}[A]^+[MO_4]^-$ are the total electronic energies of the cationic ligands $[A]^+$, metallic anions $[MO_4]^-$ and the $[A]^+[MO_4]^-$ adducts respectively. The NBO population analysis was performed using Weinhold's methodology.[6,7] The AIM and RDG methods were employed as implemented in the Multiwfn software.[8] According to Bader's[9,10] theory, the presence of a BCP between two atoms indicates bond formation. The values of certain parameters at BCPs are used to clarify the nature of the bond formed between two atoms. Espinosa et al.[11] classified the bonding interactions into three categories: (1) Pure closed-shell interactions (e.g., ionic bonds, hydrogen bonds and van der Waals interactions) characterized by $|V_{BCP}|/G_{BCP}<1$ ($\nabla^2\rho_{BCP}>0$ and $H_{BCP}>0$); (2) pure open-shell (covalent) interactions characterized by $|V_{BCP}|/G_{BCP}>2$ ($\nabla^2\rho_{BCP}<0$ and $H_{BCP}<0$); and (3) intermediate bonds with $1< |V_{BCP}|/G_{BCP}<2$ (i.e., $\nabla^2\rho_{BCP}>0$ and $H_{BCP}<0$). Finally, the RDG is defined as follows:

$$\mathrm{RDG}(r) = \frac{1}{2(3\pi^2)^{1/3}}\frac{|\nabla\rho(\rho)|}{\rho(r)^{4/3}}$$

where ρ(r) is the electron density.

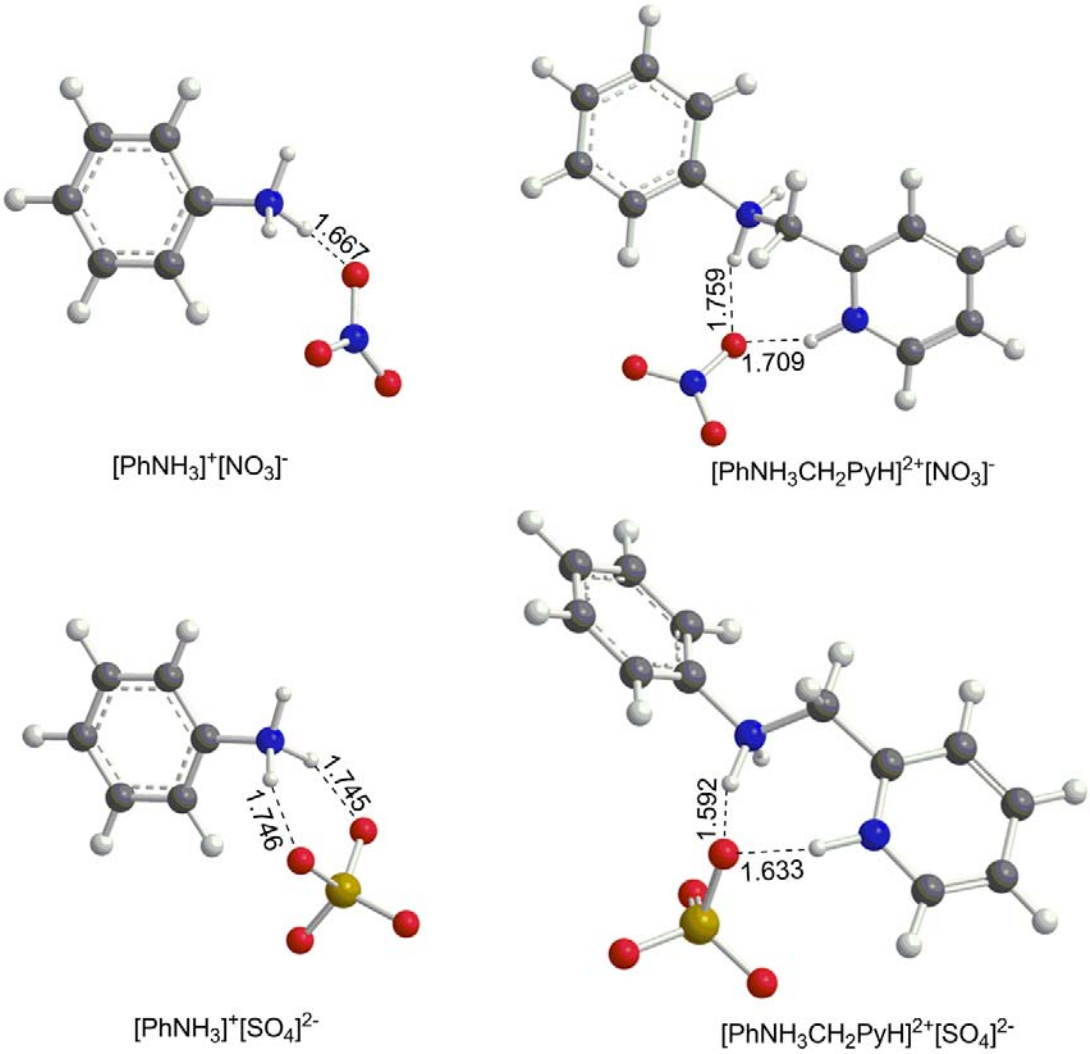

Figure S13. Optimized geometries of the adducts formed between SO_4^{2-} and NO_3^- with $[PhNH_3]^+$ and $[PhNH_2CH_2PyH]^{2+}$ ligands (distances in Å).

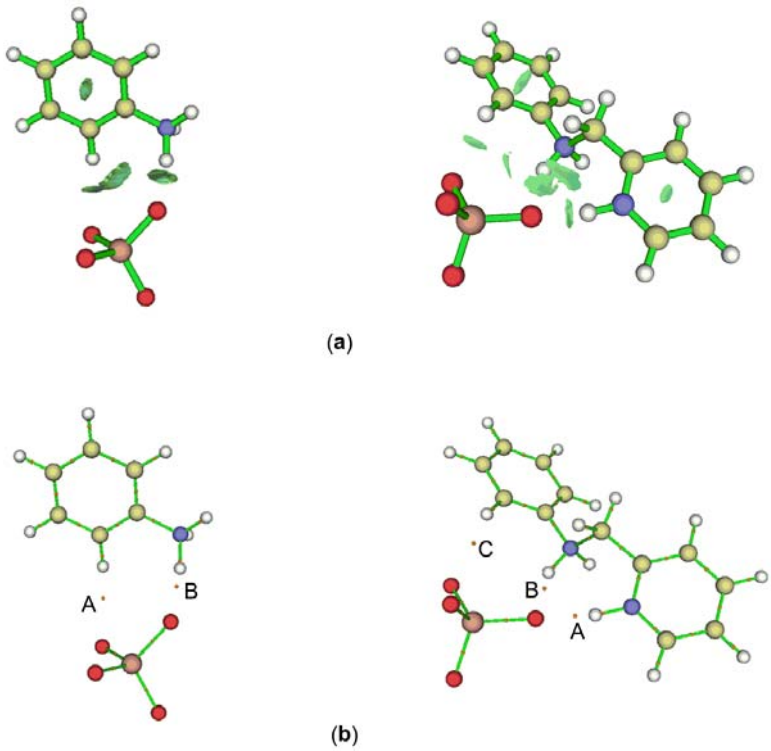

Figure S14. 3D plots of RDG (a) and BCPs derived from AIM analysis (b) for the adducts formed between anions and the cationic ligands.

Table S2. Topological and energetic properties of $\rho(\mathbf{r})$ calculated at the (3,-1) bond critical point (BCP) of the O···H interactions. The associated units in parentheses: ρ_{BCP} (eÅ^{-3}), and $\nabla^2\rho_{BCP}$ (eÅ^{-5}), G_{BCP}, V_{BCP} and H_{BCP} (in kJ/mol per atomic unit volume) and H_{BCP}/ρ_{BCP} (in kJ/mol per electron). The bond degree parameter H_{BCP}/ρ_{BCP} represents either the covalence ($H_{BCP} < 0$) or the softening ($H_{BCP} > 0$) degree of the interaction.

Parameter	$[PhNH_3]^+[TcO_4]^-$		$[PhNH_2CH_2PyH]^{2+}[TcO_4]^-$			$[PhNH_3]^+[ReO_4]^-$		$[PhNH_2CH_2PyH]^{2+}[ReO_4]^-$		
	BCP_A	BCP_B	BCP_A	BCP_B	BCP_C	BCP_A	BCP_B	BCP_A	BCP_B	BCP_C
ρ_{BCP}	0.010	0.048	0.049	0.019	0.013	0.012	0.054	0.061	0.028	0.041
$\nabla^2\rho_{BCP}$	0.036	0.165	0.171	0.062	0.045	0.043	0.185	0.207	0.088	0.152
G_{BCP}	0.008	0.042	0.043	0.016	0.010	0.010	0.047	0.055	0.023	0.038
V_{BCP}	-0.007	-0.043	-0.044	-0.016	-0.010	-0.009	-0.048	-0.058	-0.024	-0.037
$\lvert V_{BCP}\rvert/G_{BCP}$	0.875	1.024	1.023	1.000	1.000	0.900	1.021	1.055	1.043	0.974
H_{BCP}	0.001	-0.001	-0.001	-0.0002	0.001	0.001	-0.001	-0.003	-0.001	0.0003
G_{BCP}/ρ_{BCP}	0.800	0.875	0.878	0.842	0.769	0.185	0.185	0.902	0.821	0.927
H_{BCP}/ρ_{BCP}	0.100	-0.021	-0.020	-0.011	0.077	0.083	-0.019	-0.049	-0.037	0.007

Table S3. Cartesian Coordinates and selected energetic data.

TcO_4^-

Tc	0.000000000	0.000000000	0.000000000
O	0.978008000	0.978008000	0.978008000
O	-0.978008000	-0.978008000	0.978008000
O	-0.978008000	0.978008000	-0.978008000
O	0.978008000	-0.978008000	-0.978008000

Sum of electronic and zero-point Energies= -4506.978295
Sum of electronic and thermal Energies= -4506.973380
Sum of electronic and thermal Enthalpies= -4506.972436
Sum of electronic and thermal Free Energies= -4507.005167

ReO_4^-

Re	0.000000000	0.000000000	0.000000000
O	1.003664000	1.003664000	1.003664000
O	-1.003664000	-1.003664000	1.003664000
O	-1.003664000	1.003664000	-1.003664000
O	1.003664000	-1.003664000	-1.003664000

Sum of electronic and zero-point Energies= -16046.105925
Sum of electronic and thermal Energies= -16046.100252
Sum of electronic and thermal Enthalpies= -16046.099307
Sum of electronic and thermal Free Energies= -16046.134448

SO_4^{-2}

O	-0.406045000	1.325583000	-0.595377000
S	-0.000187000	-0.000046000	-0.000001000
O	0.850969000	0.237604000	1.223218000
O	0.790358000	-0.787168000	-1.016160000
O	-1.234907000	-0.775926000	0.388321000

Sum of electronic and zero-point Energies= -699.234671
Sum of electronic and thermal Energies= -699.230601
Sum of electronic and thermal Enthalpies= -699.229657
Sum of electronic and thermal Free Energies= -699.262175

NO_3^-

O	1.131264000	0.539553000	0.000014000
N	-0.000020000	0.000043000	-0.000049000
O	-0.098273000	-1.249340000	0.000014000
O	-1.032974000	0.709750000	0.000014000

Sum of electronic and zero-point Energies= -280.370253
Sum of electronic and thermal Energies= -280.367112
Sum of electronic and thermal Enthalpies= -280.366168
Sum of electronic and thermal Free Energies= -280.395728

$[PhNH_3]^+[TcO_4]^-$

Tc	-1.939572000	-0.097783000	-0.076819000
O	-3.519822000	0.440459000	0.186960000
O	-1.897693000	-1.147288000	-1.400363000
O	-0.920950000	1.239701000	-0.401361000
O	-1.389706000	-0.912572000	1.299167000
N	1.525912000	2.006164000	0.443679000
H	0.542083000	1.802578000	0.126194000
H	1.863650000	2.818314000	-0.077834000
H	1.488399000	2.277461000	1.430250000
C	2.377345000	0.827964000	0.236374000
C	1.943156000	-0.390669000	0.744800000

H	1.001709000	-0.468503000	1.281900000
C	3.566195000	0.955810000	-0.467958000
H	3.882108000	1.917998000	-0.860426000
C	3.940684000	-1.412086000	-0.158435000
H	4.555068000	-2.293382000	-0.313764000
C	2.739141000	-1.515589000	0.543249000
H	2.414853000	-2.474854000	0.933790000
C	4.352294000	-0.179575000	-0.662496000
H	5.284817000	-0.095617000	-1.211081000

Sum of electronic and zero-point Energies= -4794.818648
Sum of electronic and thermal Energies= -4794.806848
Sum of electronic and thermal Enthalpies= -4794.805904
Sum of electronic and thermal Free Energies= -4794.858460

$[PhNH_3]^+[ReO_4]^-$

Re	-1.676579000	-0.056392000	-0.000931000
O	-3.149412000	0.828808000	0.188166000
O	-1.850219000	-1.154550000	-1.329459000
O	-0.354721000	1.062125000	-0.277121000
O	-1.355143000	-0.942398000	1.450411000
N	2.132272000	1.963560000	-0.016760000
H	1.124345000	1.679022000	-0.154141000
H	2.379009000	2.616630000	-0.764483000
H	2.187277000	2.482579000	0.863899000
C	3.015260000	0.788594000	-0.005727000
C	2.443036000	-0.476609000	-0.006673000
H	1.366549000	-0.584846000	-0.006642000
C	4.391776000	0.978230000	0.003764000
H	4.814118000	1.978821000	0.008550000
C	4.669128000	-1.422243000	0.001794000
H	5.318870000	-2.291789000	0.001199000
C	3.285362000	-1.586985000	-0.006331000
H	2.851628000	-2.581503000	-0.013389000
C	5.221030000	-0.140656000	0.009536000
H	6.298101000	-0.008288000	0.018027000

Sum of electronic and zero-point Energies= -16333.949091
Sum of electronic and thermal Energies= -16333.937637
Sum of electronic and thermal Enthalpies= -16333.936692
Sum of electronic and thermal Free Energies= -16333.988123

$[PhNH_3]^+[SO_4]^{-2}$

O	2.127118000	-1.619309000	-0.000513000
S	2.404229000	-0.148985000	0.000165000
O	1.763888000	0.484483000	-1.226937000
O	3.871866000	0.123618000	0.000120000
O	1.763454000	0.483535000	1.227553000
N	-0.390749000	1.488867000	-0.000322000
C	-1.576108000	0.641364000	-0.000139000
C	-2.841885000	1.212183000	0.000168000
C	-3.957847000	0.375852000	0.000263000
C	-3.797047000	-1.008366000	0.000098000
C	-2.516204000	-1.561693000	-0.000215000
C	-1.393098000	-0.738173000	-0.000301000
H	0.262204000	1.260330000	-0.793248000
H	0.261669000	1.261502000	0.793172000
H	-0.611859000	2.484407000	-0.001267000
H	-2.964191000	2.291548000	0.000211000

H	-4.951863000	0.811786000	0.000459000
H	-4.668489000	-1.655802000	0.000195000
H	-2.387503000	-2.639611000	-0.000372000
H	-0.389870000	-1.158074000	-0.000571000

Sum of electronic and zero-point Energies= -987.092719
Sum of electronic and thermal Energies= -987.081415
Sum of electronic and thermal Enthalpies= -987.080470
Sum of electronic and thermal Free Energies= -987.133131

$[PhNH_3]^+[NO_3]^-$

N	0.063844000	1.500760000	0.514575000
C	-1.078256000	0.621145000	0.247934000
C	-0.900601000	-0.747994000	0.408290000
C	-1.975597000	-1.594494000	0.150632000
C	-3.199887000	-1.069798000	-0.264426000
C	-3.353351000	0.306074000	-0.422737000
C	-2.285706000	1.165527000	-0.165783000
H	-0.149669000	2.477854000	0.305208000
H	0.909054000	1.209862000	-0.058735000
H	0.060058000	-1.139424000	0.730534000
H	-1.853362000	-2.665870000	0.273150000
H	-4.034249000	-1.734584000	-0.464835000
H	-4.303880000	0.717572000	-0.746502000
H	-2.401117000	2.238688000	-0.287106000
H	0.353292000	1.455349000	1.495223000
O	2.421150000	-0.343445000	1.022888000
N	2.840817000	-0.175690000	-0.141462000
O	2.202130000	0.602591000	-0.917587000
O	3.857675000	-0.748858000	-0.553075000

Sum of electronic and zero-point Energies= -568.214924
Sum of electronic and thermal Energies= -568.204435
Sum of electronic and thermal Enthalpies= -568.203491
Sum of electronic and thermal Free Energies= -568.254389

$[PhNH_2CH_2PyH]^{2+}[TcO_4]^-$

Tc	-2.429357000	-0.977751000	-0.035167000
O	-0.758584000	-1.394904000	-0.114233000
O	-3.016405000	-1.325053000	1.508845000
O	-2.588996000	0.680039000	-0.328527000
O	-3.308558000	-1.852446000	-1.183979000
N	1.107834000	0.931458000	-0.452159000
C	0.831855000	2.370060000	-0.264437000
C	-0.315092000	2.762348000	0.407882000
C	-0.524811000	4.124609000	0.608482000
C	0.398629000	5.057274000	0.142104000
C	1.544832000	4.634563000	-0.528663000
C	1.771297000	3.277440000	-0.735065000
C	1.824061000	0.321873000	0.731205000
C	2.559176000	-0.941667000	0.377063000
C	3.936190000	-1.038188000	0.401595000
C	2.381437000	-3.217561000	-0.245567000
C	4.539535000	-2.261721000	0.106084000
C	3.757210000	-3.362882000	-0.218256000
N	1.833112000	-2.034165000	0.051900000
H	1.665232000	0.809555000	-1.303938000
H	0.235196000	0.402853000	-0.607181000

H	-1.045015000	2.036874000	0.751854000
H	-1.420604000	4.452709000	1.124729000
H	0.223936000	6.116562000	0.298899000
H	2.264931000	5.357944000	-0.895231000
H	2.662653000	2.939394000	-1.254619000
H	1.067022000	0.146413000	1.496300000
H	2.530370000	1.064310000	1.097531000
H	4.531587000	-0.171441000	0.660965000
H	1.696847000	-4.017530000	-0.494030000
H	5.619706000	-2.347808000	0.131649000
H	4.198696000	-4.323272000	-0.450952000
H	0.799591000	-1.922295000	0.006605000

Sum of electronic and zero-point Energies= -5081.459064
Sum of electronic and thermal Energies= -5081.441674
Sum of electronic and thermal Enthalpies= -5081.440730
Sum of electronic and thermal Free Energies= -5081.507018

$[PhNH_2CH_2PyH]^{2+}[ReO_4]^-$

symmetry c1

Re	-2.143243000	-0.475260000	-0.018616000
O	-0.387795000	-0.903551000	0.169017000
O	-2.943220000	-1.042978000	1.457740000
O	-2.069600000	1.314657000	-0.098951000
O	-3.044599000	-1.118812000	-1.405012000
N	1.803929000	0.828999000	-0.536358000
C	1.608915000	2.271124000	-0.313241000
C	0.359865000	2.704858000	0.138609000
C	0.190063000	4.063783000	0.401707000
C	1.267762000	4.944949000	0.224212000
C	2.511729000	4.493050000	-0.242566000
C	2.698336000	3.136814000	-0.519586000
C	2.586122000	0.204924000	0.601648000
C	2.943455000	-1.233624000	0.307021000
C	4.252162000	-1.701513000	0.283401000
C	2.108904000	-3.392173000	-0.159584000
C	4.472358000	-3.058377000	0.023304000
C	3.402634000	-3.908230000	-0.205405000
N	1.931386000	-2.098925000	0.101935000
H	2.267882000	0.645185000	-1.433514000
H	0.869993000	0.357062000	-0.570687000
H	-0.489386000	2.005532000	0.196698000
H	-0.792707000	4.414211000	0.757955000
H	1.134028000	6.002920000	0.449887000
H	3.345346000	5.194184000	-0.395357000
H	3.667696000	2.777508000	-0.888542000
H	1.959221000	0.279061000	1.497499000
H	3.495457000	0.798719000	0.764804000
H	5.079768000	-1.016379000	0.445638000
H	1.214447000	-3.985524000	-0.322726000
H	5.487726000	-3.426114000	-0.003091000
H	3.548594000	-4.965386000	-0.408599000
H	0.955843000	-1.695027000	0.127721000

Sum of electronic and zero-point Energies= -16620.573492
Sum of electronic and thermal Energies= -16620.556287
Sum of electronic and thermal Enthalpies= -16620.555343

Sum of electronic and thermal Free Energies= -16620.619921

$[PhNH_2CH_2PyH]^{2+}[SO_4]^{-2}$

S	-0.886606000	2.454862000	-0.221414000
O	-0.483942000	1.438967000	0.891735000
O	-2.376958000	2.443330000	-0.290194000
O	-0.351932000	3.790020000	0.150128000
O	-0.273411000	1.937482000	-1.485281000
N	0.784361000	-0.581107000	-0.242310000
C	2.244986000	-0.584497000	-0.119927000
C	2.818886000	0.158841000	0.903783000
C	4.204785000	0.141808000	1.044209000
C	4.988276000	-0.608276000	0.168370000
C	4.390645000	-1.344868000	-0.854135000
C	3.005870000	-1.339609000	-1.003688000
C	0.134294000	-1.713577000	0.493493000
C	-1.359172000	-1.764214000	0.287584000
C	-2.011286000	-2.910790000	-0.128969000
C	-3.419693000	-0.611351000	0.417978000
C	-3.401034000	-2.899086000	-0.257359000
C	-4.115889000	-1.737930000	0.016552000
N	-2.088627000	-0.660874000	0.555545000
H	0.509650000	-0.584136000	-1.229059000
H	0.395322000	0.334908000	0.155179000
H	2.196430000	0.745911000	1.572839000
H	4.669344000	0.719293000	1.836771000
H	6.067887000	-0.616679000	0.280425000
H	5.000363000	-1.925003000	-1.539065000
H	2.533713000	-1.911047000	-1.797822000
H	0.372735000	-1.578652000	1.551643000
H	0.583625000	-2.645576000	0.152153000
H	-1.440265000	-3.804217000	-0.352031000
H	-3.878158000	0.346913000	0.626317000
H	-3.918361000	-3.795345000	-0.581579000
H	-5.192808000	-1.696258000	-0.086781000
H	-1.577980000	0.228849000	0.822518000

Sum of electronic and zero-point Energies= -1273.746611

Sum of electronic and thermal Energies= -1273.729883

Sum of electronic and thermal Enthalpies= -1273.728939

Sum of electronic and thermal Free Energies= -1273.793867

$[PhNH_2CH_2PyH]^{2+}[NO_3]^{-}$

N	0.544237000	-0.573804000	-0.569138000
C	1.989301000	-0.702724000	-0.312465000
C	2.697245000	0.427476000	0.071416000
C	4.057041000	0.291396000	0.345361000
C	4.675909000	-0.952309000	0.233114000
C	3.940540000	-2.071819000	-0.156695000
C	2.581062000	-1.953657000	-0.432687000
C	-0.288755000	-0.914892000	0.637936000
C	-1.758794000	-1.032490000	0.327210000
C	-2.450168000	-2.220190000	0.475118000
C	-3.749171000	0.066614000	-0.330429000
C	-3.822792000	-2.252808000	0.221584000
C	-4.481742000	-1.098262000	-0.183748000
N	-2.434877000	0.068442000	-0.070010000

H	0.278049000	-1.167559000	-1.360275000
H	0.325032000	0.413238000	-0.837357000
H	2.205851000	1.394855000	0.146872000
H	4.630350000	1.163061000	0.643513000
H	5.735449000	-1.050286000	0.447210000
H	4.422588000	-3.039436000	-0.248511000
H	2.000342000	-2.819767000	-0.736712000
H	-0.096537000	-0.135830000	1.378608000
H	0.075318000	-1.863747000	1.029484000
H	-1.922643000	-3.112619000	0.789432000
H	-4.175381000	1.008330000	-0.651297000
H	-4.369574000	-3.181616000	0.339963000
H	-5.544508000	-1.092502000	-0.389702000
H	-1.897457000	0.950280000	-0.224521000
O	-1.178467000	3.539130000	0.569658000
N	-0.276318000	2.941802000	-0.022983000
O	-0.583774000	1.915628000	-0.737204000
O	0.907713000	3.290307000	0.034285000

Sum of electronic and zero-point Energies= -854.858047
Sum of electronic and thermal Energies= -854.842371
Sum of electronic and thermal Enthalpies= -854.841427
Sum of electronic and thermal Free Energies= -854.904093

References (for computational details)

1) Frisch, M. J.; Trucks, G. W.; Schlegel, H. B.; Scuseria, G. E.; Robb,M. A.; Cheeseman, J. R.; Scalmani, G.; Barone, V.; Mennucci, B.; Petersson, G. A.; Nakatsuji, H.;Caricato, M.; Li, X.; Hratchian, H. P.; Izmaylov, A. F.; Bloino, J.; Zheng, G.; Sonnenberg, J. L.; Hada,M.; Ehara, M.; Toyota, K.; Fukuda, R.; Hasegawa, J.; Ishida, M.; Nakajima, T.; Honda, Y.; Kitao, O.;Nakai, H.; Vreven, T.; Montgomery, J. A., Jr.; Peralta, J. E.; Ogliaro, F.; Bearpark, M.; Heyd, J. J.;Brothers, E.; Kudin, K. N.; Staroverov, V. N.; Kobayashi, R.; Normand, J.; Raghavachari, K.; Rendell, A.; Burant, J. C.; Iyengar, S. S.; Tomasi, J.; Cossi, M.; Rega, N.; Millam, N. J.; Klene, M.; Knox, J. E.;Cross, J. B.; Bakken, V.; Adamo, C.; Jaramillo, J.; Gomperts, R.; Stratmann, R. E.; Yazyev, O.;Austin, A. J.; Cammi, R.; Pomelli, C.; Ochterski, J. W.; Martin, R. L.; Morokuma, K.; Zakrzewski, V. G.;Voth, G. A.; Salvador, P.; Dannenberg, J. J.; Dapprich, S.; Daniels, A. D.; Farkas, Ö.; Foresman, J. B.; Ortiz, J. V.; Cioslowski, J.; Fox, D. J. Gaussian 09, Revision D.01; Gaussian, Inc.: Wallingford, CT, 2010.

(2) J.-D. Chai and M. Head-Gordon, *J. Chem. Phys.*, *128*, **2008**, 084106.

(3) P. J. P. de Oliveira, C. L. Barros, F. E. Jorge, A. Canal Neto, and M. Campos, *J. Mol. Struct. (Theochem)*, *43*, **2010**, 948.

(4) A. Canal Neto and F. E. Jorge, *Chem. Phys. Let.*, *158*, **2013**, 582.

(5) J. Tomasi, B. Mennucci, R. Cammi, *Chem. Rev. 105*, **2005**, 2999.

(6) A. E. Reed, L. A. Curtiss, F. Weinhold, *Chem. Rev. 88*, **1988**, 899.

(7) F. Weinhold, *In The Encyclopedia of Computational Chemistry*; Schleyer, P. v. R., Ed.; John Wiley & Sons: Chichester, **1998**; pp 1792−1811.

(8) T. Lu, F. Chen, Multiwfn: A Multifunctional Wavefunction Analyzer, *J. Comp. Chem.* **33**, 580-592 (2012).

(9) R. F. W. Bader (**1990**) Atoms in molecules—a quantum theory. Oxford University Press, Oxford.

(10) R. F. W. Bader (**1998**) *J Phys Chem* A *102*, 7314.

(11) E. Espinosa, I. Alkorta, J. Elguero, E. Molins E (**2002**) *J Chem Phys 117*, 5529.

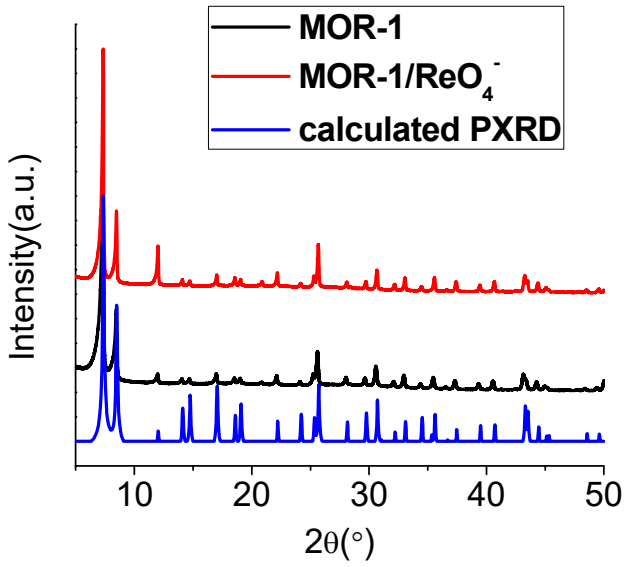

Figure S15. PXRD patterns of **MOR-1** (experimental and calculated) and **MOR-1/ReO_4^-**.

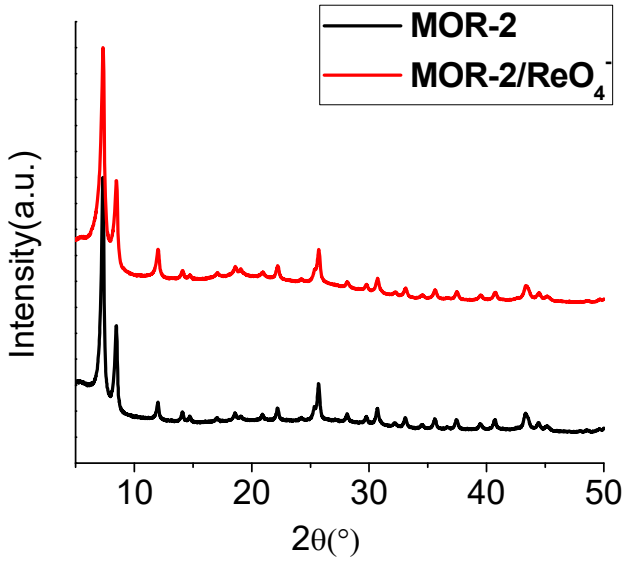

Figure S16. PXRD patterns of **MOR-2** and **MOR-2/ReO_4^-**.

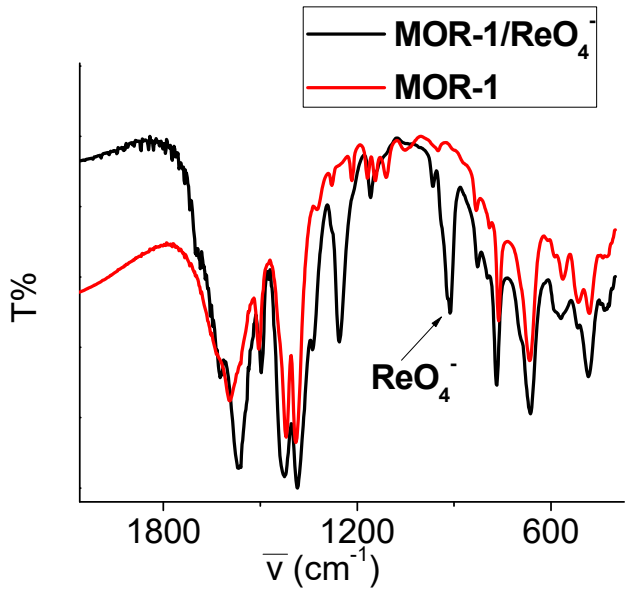

Figure S17. IR spectra of **MOR-1** and **MOR-1 /ReO_4^-**.

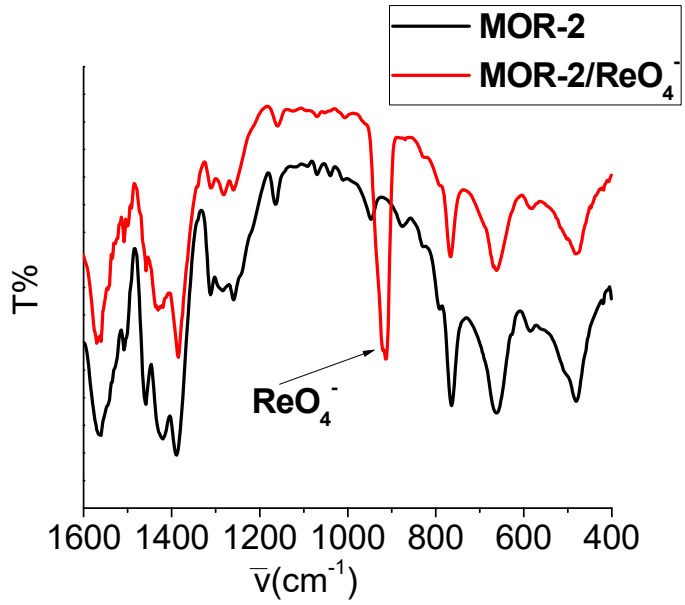

Figure S18. IR spectra of **MOR-2** and **MOR-2 /ReO_4^-**.

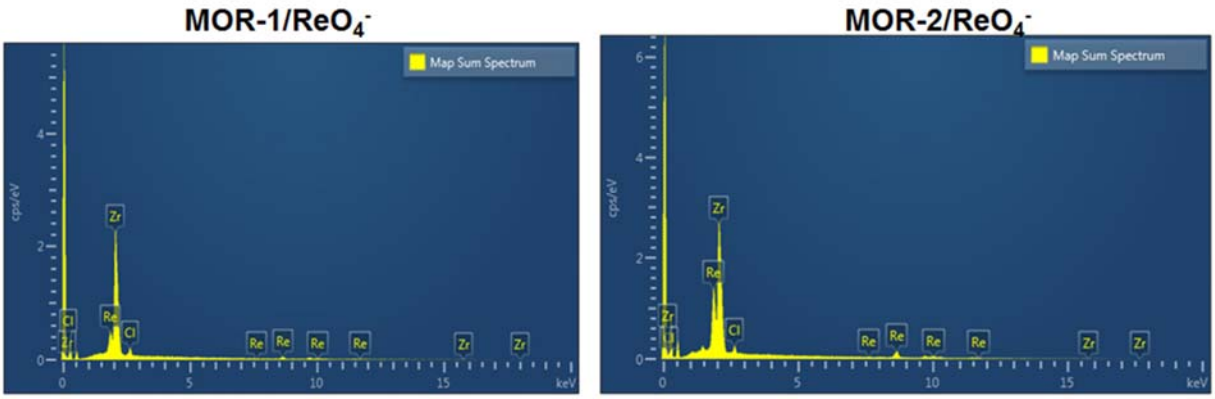

Figure S19. EDS data for the ReO_4^--loaded materials. According to ReO_4^- sorption data for **MOR-1** (see main text), there is partial exchange of Cl^- by Re(VII) species and this is confirmed by the EDS data for **MOR-1/ReO_4^-** indicating the existence of both Re and Cl. However, the ReO_4^- sorption data for **MOR-2** indicate complete exchange of guest Cl^- by ReO_4^- anions. Thus, the chloride found from the EDS data for **MOR-2/ReO_4^-** is likely attributed to Cl^- interacting

strongly with surface ammonium/pyridinium functional groups of **MOR-2** (i.e. Cl^- anions are located in the external surface of **MOR-2** particles).

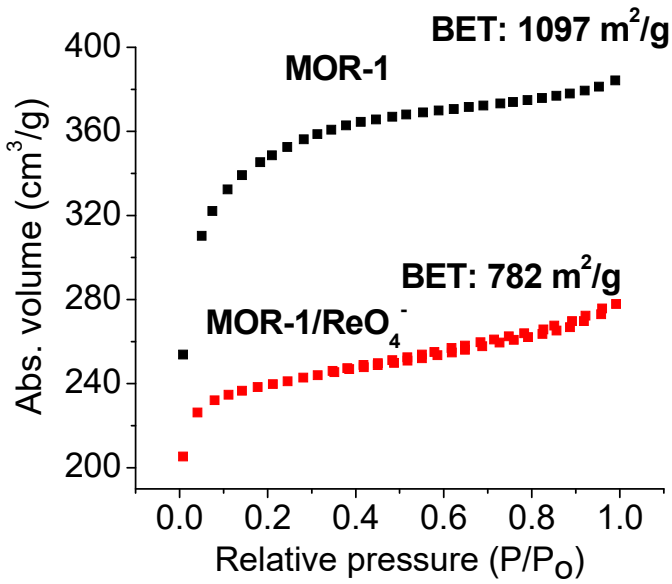

.

Figure S20. Nitrogen sorption isotherm at 77 K for **MOR-1** and **MOR-1/ReO_4^-**.

<u>Crystal structure solution and Rietveld refinement for MOR-1/ReO_4^-</u>

The X-ray powder diffraction pattern for **MOR-1** loaded with ReO_4^- was indexed with TREOR (*Fm-3m*, a = 20.7873 Å) implemented in EXPO2014 (A. Altomare, C. Cuocci, C. Giacovazzo, A. Moliterni, R. Rizzi, N. Corriero and A. Falcicchio, *J. Appl. Cryst.* (2013), **46**, 1231) to give the expected cubic unit cell. Attempts to solve the structure with direct methods resulted in the familiar Zr_6O_8 core and diffuse electron density in the cell. An interesting characteristic of the maps systematically produced is a relatively high intensity peak above a triangular face of the Zr_6O_8 octahedron at close proximity to the μ_3–O atom. This peak was assigned to Re, and a tetrahedron ReO_4 was built. Additionally, the aminoterephthalate ligand was built in agreement to previously reported structures (see for example C.A.Trickett, K.J.Gagnon, Seungkyu Lee, F.Gandara, H.-B.Burgi, O.M.Yaghi, *Angew.Chem ,Int.Ed.* (2015), **54**, 11162) and a free chloride anion was added in the structure. The occupancies of the Zr, μ_3–O, and terephthalate atoms were

assigned according to the *Fm-3m* space group demands while the occupancies of the perrhenate and chloride atoms were assigned according to analytical data. The final formula used was $\{[Zr_6O_4(OH)_4(C_8H_6NO_4)_6](ReO_4)_4Cl_2\}_n$. The structure was solved with simulated annealing methods allowing ReO_4^- to rotate about Re atom and Cl^- free to move. The final Rietveld plot is presented in Fig. S21. CIF data are given below.

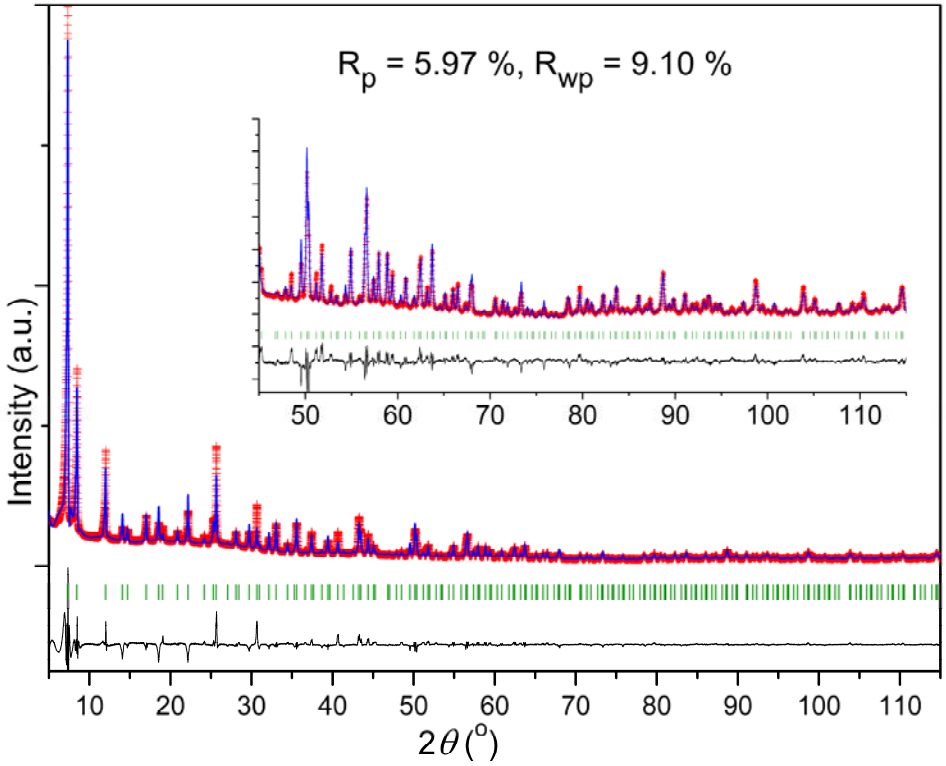

Figure S21. The final Rietveld plot for **MOR-1/ReO_4^-.**

<u>CIF data for MOR-1/ReO_4^-</u>

```
_audit_creation_method            Expo2014

_chemical_name_systematic     ?
_chemical_formula_moiety      'Re4 Zr6 Cl2 O48 N6 C48'
_chemical_formula_sum         'Re4 Zr6 Cl2 O48 N6 C48'
_chemical_formula_weight      2831.92
```

```
loop_
    _atom_type_symbol
    _atom_type_description
    _atom_type_scat_source
   'C'   'Carbon'   'International Tables Vol C Tables 4.2.6.8 and 6.1.1.4'
   'N'   'Nitrogen'   'International Tables Vol C Tables 4.2.6.8 and 6.1.1.4'
   'O'   'Oxygen'   'International Tables Vol C Tables 4.2.6.8 and 6.1.1.4'
   'Cl'   'Chlorine'   'International Tables Vol C Tables 4.2.6.8 and 6.1.1.4'
   'Zr'   'Zirconium'   'International Tables Vol C Tables 4.2.6.8 and 6.1.1.4'
   'Re'   'Rhenium'   'International Tables Vol C Tables 4.2.6.8 and 6.1.1.4'

_cell_length_a                    20.78730
_cell_length_b                    20.78730
_cell_length_c                    20.78730
_cell_angle_alpha                    90.000
_cell_angle_beta                    90.000
_cell_angle_gamma                    90.000
_cell_volume                    8982.438
_cell_formula_units_Z           4
_cell_measurement_temperature    ?

_exptl_crystal_density_diffrn        2.094
_exptl_crystal_density_meas      ?
_exptl_crystal_density_method 'not measured'
_symmetry_Int_Tables_number         225
_symmetry_cell_setting              cubic
_symmetry_space_group_name_H-M      'F m -3 m'
_symmetry_space_group_name_hall     '-F 4 2 3'

loop_
   _symmetry_equiv_pos_site_id
   _symmetry_equiv_pos_as_xyz
   1   'x, y, z'
   2   '-y, x, z'
   3   '-x, -y, z'
   4   'y, -x, z'
   5   'x, -y, -z'
   6   'y, x, -z'
   7   '-x, y, -z'
   8   '-y, -x, -z'
   9   'z, x, y'
  10   '-x, z, y'
  11   '-z, -x, y'
  12   'x, -z, y'
  13   'z, -x, -y'
```

14 'x, z, -y'
15 '-z, x, -y'
16 '-x, -z, -y'
17 'y, z, x'
18 'y, -z, -x'
19 'z, y, -x'
20 '-y, z, -x'
21 '-z, -y, -x'
22 '-y, -z, x'
23 'z, -y, x'
24 '-z, y, x'
25 '-x, -y, -z'
26 'y, -x, -z'
27 'x, y, -z'
28 '-y, x, -z'
29 '-x, y, z'
30 '-y, -x, z'
31 'x, -y, z'
32 'y, x, z'
33 '-z, -x, -y'
34 'x, -z, -y'
35 'z, x, -y'
36 '-x, z, -y'
37 '-z, x, y'
38 '-x, -z, y'
39 'z, -x, y'
40 'x, z, y'
41 '-y, -z, -x'
42 '-y, z, x'
43 '-z, -y, x'
44 'y, -z, x'
45 'z, y, x'
46 'y, z, -x'
47 '-z, y, -x'
48 'z, -y, -x'
49 'x, y+1/2, z+1/2'
50 '-y, x+1/2, z+1/2'
51 '-x, -y+1/2, z+1/2'
52 'y, -x+1/2, z+1/2'
53 'x, -y+1/2, -z+1/2'
54 'y, x+1/2, -z+1/2'
55 '-x, y+1/2, -z+1/2'
56 '-y, -x+1/2, -z+1/2'
57 'z, x+1/2, y+1/2'
58 '-x, z+1/2, y+1/2'
59 '-z, -x+1/2, y+1/2'

60 'x, -z+1/2, y+1/2'
61 'z, -x+1/2, -y+1/2'
62 'x, z+1/2, -y+1/2'
63 '-z, x+1/2, -y+1/2'
64 '-x, -z+1/2, -y+1/2'
65 'y, z+1/2, x+1/2'
66 'y, -z+1/2, -x+1/2'
67 'z, y+1/2, -x+1/2'
68 '-y, z+1/2, -x+1/2'
69 '-z, -y+1/2, -x+1/2'
70 '-y, -z+1/2, x+1/2'
71 'z, -y+1/2, x+1/2'
72 '-z, y+1/2, x+1/2'
73 '-x, -y+1/2, -z+1/2'
74 'y, -x+1/2, -z+1/2'
75 'x, y+1/2, -z+1/2'
76 '-y, x+1/2, -z+1/2'
77 '-x, y+1/2, z+1/2'
78 '-y, -x+1/2, z+1/2'
79 'x, -y+1/2, z+1/2'
80 'y, x+1/2, z+1/2'
81 '-z, -x+1/2, -y+1/2'
82 'x, -z+1/2, -y+1/2'
83 'z, x+1/2, -y+1/2'
84 '-x, z+1/2, -y+1/2'
85 '-z, x+1/2, y+1/2'
86 '-x, -z+1/2, y+1/2'
87 'z, -x+1/2, y+1/2'
88 'x, z+1/2, y+1/2'
89 '-y, -z+1/2, -x+1/2'
90 '-y, z+1/2, x+1/2'
91 '-z, -y+1/2, x+1/2'
92 'y, -z+1/2, x+1/2'
93 'z, y+1/2, x+1/2'
94 'y, z+1/2, -x+1/2'
95 '-z, y+1/2, -x+1/2'
96 'z, -y+1/2, -x+1/2'
97 'x+1/2, y, z+1/2'
98 '-y+1/2, x, z+1/2'
99 '-x+1/2, -y, z+1/2'
100 'y+1/2, -x, z+1/2'
101 'x+1/2, -y, -z+1/2'
102 'y+1/2, x, -z+1/2'
103 '-x+1/2, y, -z+1/2'
104 '-y+1/2, -x, -z+1/2'
105 'z+1/2, x, y+1/2'

106 '-x+1/2, z, y+1/2'
107 '-z+1/2, -x, y+1/2'
108 'x+1/2, -z, y+1/2'
109 'z+1/2, -x, -y+1/2'
110 'x+1/2, z, -y+1/2'
111 '-z+1/2, x, -y+1/2'
112 '-x+1/2, -z, -y+1/2'
113 'y+1/2, z, x+1/2'
114 'y+1/2, -z, -x+1/2'
115 'z+1/2, y, -x+1/2'
116 '-y+1/2, z, -x+1/2'
117 '-z+1/2, -y, -x+1/2'
118 '-y+1/2, -z, x+1/2'
119 'z+1/2, -y, x+1/2'
120 '-z+1/2, y, x+1/2'
121 '-x+1/2, -y, -z+1/2'
122 'y+1/2, -x, -z+1/2'
123 'x+1/2, y, -z+1/2'
124 '-y+1/2, x, -z+1/2'
125 '-x+1/2, y, z+1/2'
126 '-y+1/2, -x, z+1/2'
127 'x+1/2, -y, z+1/2'
128 'y+1/2, x, z+1/2'
129 '-z+1/2, -x, -y+1/2'
130 'x+1/2, -z, -y+1/2'
131 'z+1/2, x, -y+1/2'
132 '-x+1/2, z, -y+1/2'
133 '-z+1/2, x, y+1/2'
134 '-x+1/2, -z, y+1/2'
135 'z+1/2, -x, y+1/2'
136 'x+1/2, z, y+1/2'
137 '-y+1/2, -z, -x+1/2'
138 '-y+1/2, z, x+1/2'
139 '-z+1/2, -y, x+1/2'
140 'y+1/2, -z, x+1/2'
141 'z+1/2, y, x+1/2'
142 'y+1/2, z, -x+1/2'
143 '-z+1/2, y, -x+1/2'
144 'z+1/2, -y, -x+1/2'
145 'x+1/2, y+1/2, z'
146 '-y+1/2, x+1/2, z'
147 '-x+1/2, -y+1/2, z'
148 'y+1/2, -x+1/2, z'
149 'x+1/2, -y+1/2, -z'
150 'y+1/2, x+1/2, -z'
151 '-x+1/2, y+1/2, -z'

```
  152   '-y+1/2, -x+1/2, -z'
  153   'z+1/2, x+1/2, y'
  154   '-x+1/2, z+1/2, y'
  155   '-z+1/2, -x+1/2, y'
  156   'x+1/2, -z+1/2, y'
  157   'z+1/2, -x+1/2, -y'
  158   'x+1/2, z+1/2, -y'
  159   '-z+1/2, x+1/2, -y'
  160   '-x+1/2, -z+1/2, -y'
  161   'y+1/2, z+1/2, x'
  162   'y+1/2, -z+1/2, -x'
  163   'z+1/2, y+1/2, -x'
  164   '-y+1/2, z+1/2, -x'
  165   '-z+1/2, -y+1/2, -x'
  166   '-y+1/2, -z+1/2, x'
  167   'z+1/2, -y+1/2, x'
  168   '-z+1/2, y+1/2, x'
  169   '-x+1/2, -y+1/2, -z'
  170   'y+1/2, -x+1/2, -z'
  171   'x+1/2, y+1/2, -z'
  172   '-y+1/2, x+1/2, -z'
  173   '-x+1/2, y+1/2, z'
  174   '-y+1/2, -x+1/2, z'
  175   'x+1/2, -y+1/2, z'
  176   'y+1/2, x+1/2, z'
  177   '-z+1/2, -x+1/2, -y'
  178   'x+1/2, -z+1/2, -y'
  179   'z+1/2, x+1/2, -y'
  180   '-x+1/2, z+1/2, -y'
  181   '-z+1/2, x+1/2, y'
  182   '-x+1/2, -z+1/2, y'
  183   'z+1/2, -x+1/2, y'
  184   'x+1/2, z+1/2, y'
  185   '-y+1/2, -z+1/2, -x'
  186   '-y+1/2, z+1/2, x'
  187   '-z+1/2, -y+1/2, x'
  188   'y+1/2, -z+1/2, x'
  189   'z+1/2, y+1/2, x'
  190   'y+1/2, z+1/2, -x'
  191   '-z+1/2, y+1/2, -x'
  192   'z+1/2, -y+1/2, -x'

loop_
   _atom_site_type_symbol
   _atom_site_label
   _atom_site_fract_x
```

```
   _atom_site_fract_y
   _atom_site_fract_z
   _atom_site_U_iso_or_equiv
   _atom_site_occupancy
   _atom_site_adp_type
Zr      Zr      0.1205 0.0000 0.0000 0.0500 0.12500      Uiso
O       O2      0.0628 0.0628 0.0628 0.0800 0.16667      Uiso
Re      Re1     0.1480 0.1480 0.1480 0.0800 0.08333      Uiso
O       O4      0.1960 0.1960 0.1960 0.1000 0.08333      Uiso
O       O1      0.1805 0.0000 0.0848 0.0800 0.25000      Uiso
C       C3      0.2674 0.0000 0.1844 0.1000 0.50000      Uiso
N       N       0.2842 0.0000 0.1217 0.1000 0.12500      Uiso
C       C1      0.1536 0.0000 0.1536 0.1000 0.25000      Uiso
C       C2      0.2050 0.0000 0.2050 0.1000 0.25000      Uiso
O       O3      0.2040 0.0919 0.0919 0.1000 0.25000      Uiso
Cl      Cl1     0.2875 0.1258 0.1258 0.1000 0.04167      Uiso

loop_
   _geom_bond_atom_site_label_1
   _geom_bond_atom_site_label_2
   _geom_bond_distance
   _geom_bond_site_symmetry_2
Zr O2  2.201114 .
Zr O1  2.158924 .
Re1 O4  1.727503 .
Re1 O3  2.018182 .
O1 C1  1.535209 .
C3 N  1.349084 .
C3 C2  1.367695 .
C1 C2  1.510747 .

loop_
_geom_angle_atom_site_label_1
_geom_angle_atom_site_label_2
_geom_angle_atom_site_label_3
_geom_angle
_geom_angle_site_symmetry_1
_geom_angle_site_symmetry_3
O2 Zr O1    80.25 . .
Zr O1 C1   123.36 . .
O4 Re1 O3   109.52 . .
O1 C1 C2   113.64 . .
N C3 C2   123.23 . .
C3 C2 C1   116.76 . .

loop_
```

```
    _geom_torsion_atom_site_label_1
    _geom_torsion_atom_site_label_2
    _geom_torsion_atom_site_label_3
    _geom_torsion_atom_site_label_4
    _geom_torsion
    _geom_torsion_site_symmetry_1
    _geom_torsion_site_symmetry_2
    _geom_torsion_site_symmetry_3
    _geom_torsion_site_symmetry_4
  O2 Zr O1 C1    36.99 . . . .
  Zr O1 C1 C2  -180.00 . . . .
  N C3 C2 C1     0.00 . . . .
O1 C1 C2 C3     0.00 . . . .
```

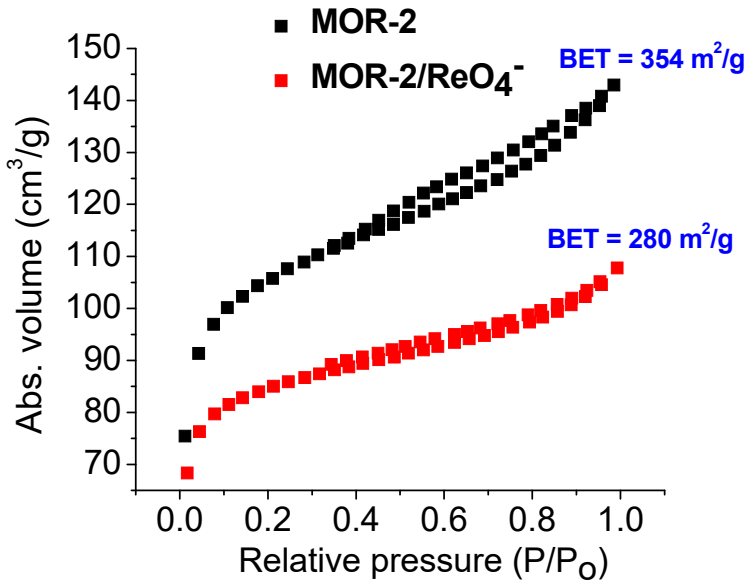

Figure S22. Nitrogen sorption isotherm at 77 K for **MOR-2** and **MOR-2 /ReO_4^-**.

<u>Crystal structure solution and Rietveld refinement for MOR-2/ReO_4^-</u>

For **MOR-2/ReO_4^-** structure, three different models were built based on the known structure of **MOR-2** (reference 19 in main article) and the amount of sorbed Re content found experimentally (sorption isotherms) which led to a formulation $\{[Zr_6O_8(C_{14}H_{12}N_2O_4)_4](ReO_4)_8\}_n$: In all cases the coordinated water molecules from the equatorial sites and chloride counter ions were removed and replaced with (a) four chelated perrhenates on the equatorial Zr atoms of the eight connected

node and four perrhenates as counter ions in the cells empty space, (b) four ReO_4^- anions acting as bridging ligands on the Zr – Zr equatorial edges and again four perrhenates as counter ions in the cells empty space, and (c) eight unidentate perrhenates on the positions of the water molecules of the original structure. We attempted to solve the structures for all three models allowing the bond distances, angles and torsions related to the bonded perrhenates to vary, the anionic perrhenates free to move and, additionally, the torsions related to aminomethylpyridine moiety were also allowed to vary. The best solutions were obtained for the third model (c), and here is presented the one that gave the best Rietveld refinement results (Fig. S22 and Fig. 7 in main article). CIF data are given below.

Here, we do not claim that the structures presented are crystallographically perfectly correct, but chemically they represent realistic models of the interactions of perrhenates with the two MOR materials.

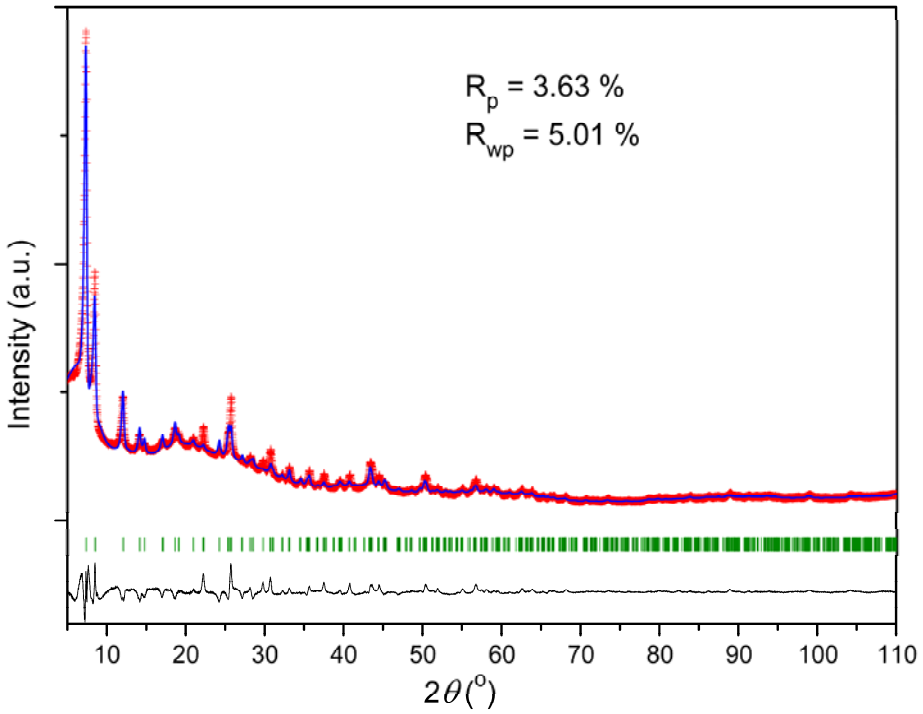

Figure S23. The final Rietveld plot for **MOR-2/ReO_4^-.**

CIF data for MOR-2/ReO_4^-

```
_audit_creation_method            Expo2014

_chemical_name_systematic     ?
_chemical_formula_moiety      'Re8 Zr6 O56 N8 C56'
_chemical_formula_sum         'Re8 Zr6 O56 N8 C56'
_chemical_formula_weight      3766.00

loop_
    _atom_type_symbol
    _atom_type_description
    _atom_type_scat_source
   'C'   'Carbon'   'International Tables Vol C Tables 4.2.6.8 and 6.1.1.4'
   'N'   'Nitrogen'   'International Tables Vol C Tables 4.2.6.8 and 6.1.1.4'
   'O'   'Oxygen'   'International Tables Vol C Tables 4.2.6.8 and 6.1.1.4'
   'Zr'   'Zirconium'   'International Tables Vol C Tables 4.2.6.8 and 6.1.1.4'
   'Re'   'Rhenium'   'International Tables Vol C Tables 4.2.6.8 and 6.1.1.4'

_cell_length_a                    14.69280
_cell_length_b                    14.69280
_cell_length_c                    20.87750
_cell_angle_alpha                    90.000
_cell_angle_beta                     90.000
_cell_angle_gamma                       90.000
_cell_volume                      4507.000
_cell_formula_units_Z          2
_cell_measurement_temperature    ?

_exptl_crystal_density_diffrn        2.775
_exptl_crystal_density_meas      ?
_exptl_crystal_density_method 'not measured'
_symmetry_Int_Tables_number         87
_symmetry_cell_setting              tetragonal
_symmetry_space_group_name_H-M      'I 4/m'
_symmetry_space_group_name_hall     '-I 4'

loop_
   _symmetry_equiv_pos_site_id
```

```
  _symmetry_equiv_pos_as_xyz
   1   'x, y, z'
   2   '-y, x, z'
   3   '-x, -y, z'
   4   'y, -x, z'
   5   '-x, -y, -z'
   6   'y, -x, -z'
   7   'x, y, -z'
   8   '-y, x, -z'
   9   'x+1/2, y+1/2, z+1/2'
  10   '-y+1/2, x+1/2, z+1/2'
  11   '-x+1/2, -y+1/2, z+1/2'
  12   'y+1/2, -x+1/2, z+1/2'
  13   '-x+1/2, -y+1/2, -z+1/2'
  14   'y+1/2, -x+1/2, -z+1/2'
  15   'x+1/2, y+1/2, -z+1/2'
  16   '-y+1/2, x+1/2, -z+1/2'

loop_
  _atom_site_type_symbol
  _atom_site_label
  _atom_site_fract_x
  _atom_site_fract_y
  _atom_site_fract_z
  _atom_site_U_iso_or_equiv
  _atom_site_occupancy
  _atom_site_adp_type
O     O1     -0.0011 0.1324 0.0628 0.0050 1.0000     Uiso
O     O2     0.1699 0.1699 0.0949 0.0800 1.0000     Uiso
O     O3     0.0950 0.0950 0.1697 0.0800 1.0000     Uiso
C     C1     0.1533 0.1533 0.1531 0.0800 1.0000     Uiso
C     C2     0.2020 0.2020 0.2007 0.0800 1.0000     Uiso
C     C3     0.1969 0.1760 0.2649 0.0800 1.0000     Uiso
C     C4     0.2552 0.2762 0.1833 0.0800 1.0000     Uiso
N     N1     0.2825 0.2982 0.1195 0.1000 0.50000    Uiso
C     C5     0.3819 0.3040 0.1115 0.1000 0.50000    Uiso
C     C6     0.4313 0.2949 0.1749 0.1000 0.50000    Uiso
C     C7     0.4487 0.3720 0.2086 0.1000 0.50000    Uiso
N     N2     0.4584 0.2109 0.2008 0.1000 0.50000    Uiso
C     C8     0.5025 0.2093 0.2598 0.1000 0.50000    Uiso
```

```
C     C9     0.5201 0.2907 0.2931 0.1000 0.50000    Uiso
C     C10    0.4915 0.3719 0.2658 0.1000 0.50000    Uiso
Re    Re1    0.1314 0.3680 0.0276 0.0800 0.50000    Uiso
O     O15    0.0441 0.4465 0.0315 0.1000 0.50000    Uiso
O     O16    0.0900 0.2646 0.0059 0.1000 0.50000    Uiso
O     O17    0.1841 0.3602 0.1021 0.1000 0.50000    Uiso
O     O18    0.2103 0.4024 -0.0283 0.1000 0.50000   Uiso
Re    Re2    -0.1224 0.3747 0.0142 0.0800 0.50000   Uiso
O     O5     -0.2103 0.4061 -0.0361 0.1000 0.50000  Uiso
O     O7     -0.0297 0.4463 0.0017 0.1000 0.50000   Uiso
O     O8     -0.1571 0.3841 0.0927 0.1000 0.50000   Uiso
O     O6     -0.0918 0.2652 0.0000 0.1000 0.50000   Uiso
Zr    Zr1    0.1195 0.1195 0.0000 0.0500 0.50000    Uiso
Zr    Zr2    0.0000 0.0000 0.1194 0.0500 0.25000    Uiso

loop_
   _geom_bond_atom_site_label_1
   _geom_bond_atom_site_label_2
   _geom_bond_distance
   _geom_bond_site_symmetry_2
O1 Zr1  2.213421 .
O1 Zr2  2.275945 .
O2 C1  1.262819 .
O2 Zr1  2.240653 .
O3 C1  1.259804 .
O3 Zr2  2.236410 .
C1 C2  1.418587 .
C2 C3  1.395051 .
C2 C4  1.390938 .
C4 N1  1.427875 .
N1 C5  1.473369 .
C5 C6  1.514764 .
C6 C7  1.357306 .
C6 N2  1.405153 .
C7 C10  1.349909 .
N2 C8  1.393615 .
C8 C9  1.406721 .
C9 C10  1.387791 .
Re1 O15  1.726419 .
Re1 O16  1.697958 .
```

```
Re1 O17  1.741611 .
Re1 O18  1.722478 .
O16 Zr1  2.177979 .
Re2 O5  1.726577 .
Re2 O7  1.741608 .
Re2 O8  1.722434 .
Re2 O6  1.697370 .

loop_
_geom_angle_atom_site_label_1
_geom_angle_atom_site_label_2
_geom_angle_atom_site_label_3
_geom_angle
_geom_angle_site_symmetry_1
_geom_angle_site_symmetry_3
Zr1 O1 Zr2   103.22 . .
O1 Zr1 O2    73.31 . .
O1 Zr1 O16    73.94 . .
O1 Zr2 O3    73.44 . .
C1 O2 Zr1   136.23 . .
O2 C1 O3   121.95 . .
O2 C1 C2   118.61 . .
O2 Zr1 O16    72.10 . .
C1 O3 Zr2   135.94 . .
O3 C1 C2   119.45 . .
C1 C2 C3   120.58 . .
C1 C2 C4   119.71 . .
C3 C2 C4   119.70 . .
C2 C4 N1   125.39 . .
C4 N1 C5   113.37 . .
N1 C5 C6   111.80 . .
C5 C6 C7   118.04 . .
C5 C6 N2   123.26 . .
C7 C6 N2   118.69 . .
C6 C7 C10   123.11 . .
C6 N2 C8   119.14 . .
C7 C10 C9   120.30 . .
N2 C8 C9   120.52 . .
C8 C9 C10   118.24 . .
O15 Re1 O16   110.16 . .
```

```
O15 Re1 O17   109.38 . .
O15 Re1 O18   109.65 . .
O16 Re1 O17   109.80 . .
O16 Re1 O18   108.86 . .
Re1 O16 Zr1   145.00 . .
O17 Re1 O18   108.96 . .
O5 Re2 O7   109.38 . .
O5 Re2 O8   109.65 . .
O5 Re2 O6   110.25 . .
O7 Re2 O8   108.97 . .
O7 Re2 O6   109.83 . .
O8 Re2 O6   108.75 . .

loop_
   _geom_torsion_atom_site_label_1
   _geom_torsion_atom_site_label_2
   _geom_torsion_atom_site_label_3
   _geom_torsion_atom_site_label_4
   _geom_torsion
   _geom_torsion_site_symmetry_1
   _geom_torsion_site_symmetry_2
   _geom_torsion_site_symmetry_3
   _geom_torsion_site_symmetry_4
Zr2 O1 Zr1 O2   -83.03 . . . .
Zr2 O1 Zr1 O16  -158.70 . . . .
Zr1 O1 Zr2 O3    83.65 . . . .
Zr1 O2 C1 O3      0.02 . . . .
Zr1 O2 C1 C2   179.98 . . . .
C1 O2 Zr1 O1    40.87 . . . .
C1 O2 Zr1 O16   118.95 . . . .
Zr2 O3 C1 O2      0.00 . . . .
Zr2 O3 C1 C2  -180.00 . . . .
C1 O3 Zr2 O1   -39.49 . . . .
O2 C1 C2 C3  -169.59 . . . .
O2 C1 C2 C4    10.40 . . . .
O3 C1 C2 C3    10.41 . . . .
O3 C1 C2 C4  -169.60 . . . .
C1 C2 C4 N1   -14.45 . . . .
C3 C2 C4 N1   165.54 . . . .
C2 C4 N1 C5  -122.59 . . . .
```

C4 N1 C5 C6 -6.04 . . . .
N1 C5 C6 C7 -90.17 . . . .
N1 C5 C6 N2 88.75 . . . .
C5 C6 C7 C10 179.36 . . . .
N2 C6 C7 C10 0.40 . . . .
C5 C6 N2 C8 -179.21 . . . .
C7 C6 N2 C8 -0.30 . . . .
C6 C7 C10 C9 0.06 . . . .
C6 N2 C8 C9 -0.23 . . . .
N2 C8 C9 C10 0.67 . . . .
C8 C9 C10 C7 -0.59 . . . .
O15 Re1 O16 Zr1 -165.75 . . . .
O17 Re1 O16 Zr1 -45.22 . . . .
O18 Re1 O16 Zr1 73.98 . . . .
Re1 O16 Zr1 O1 120.39 . . . .
Re1 O16 Zr1 O2 43.16 . . . .

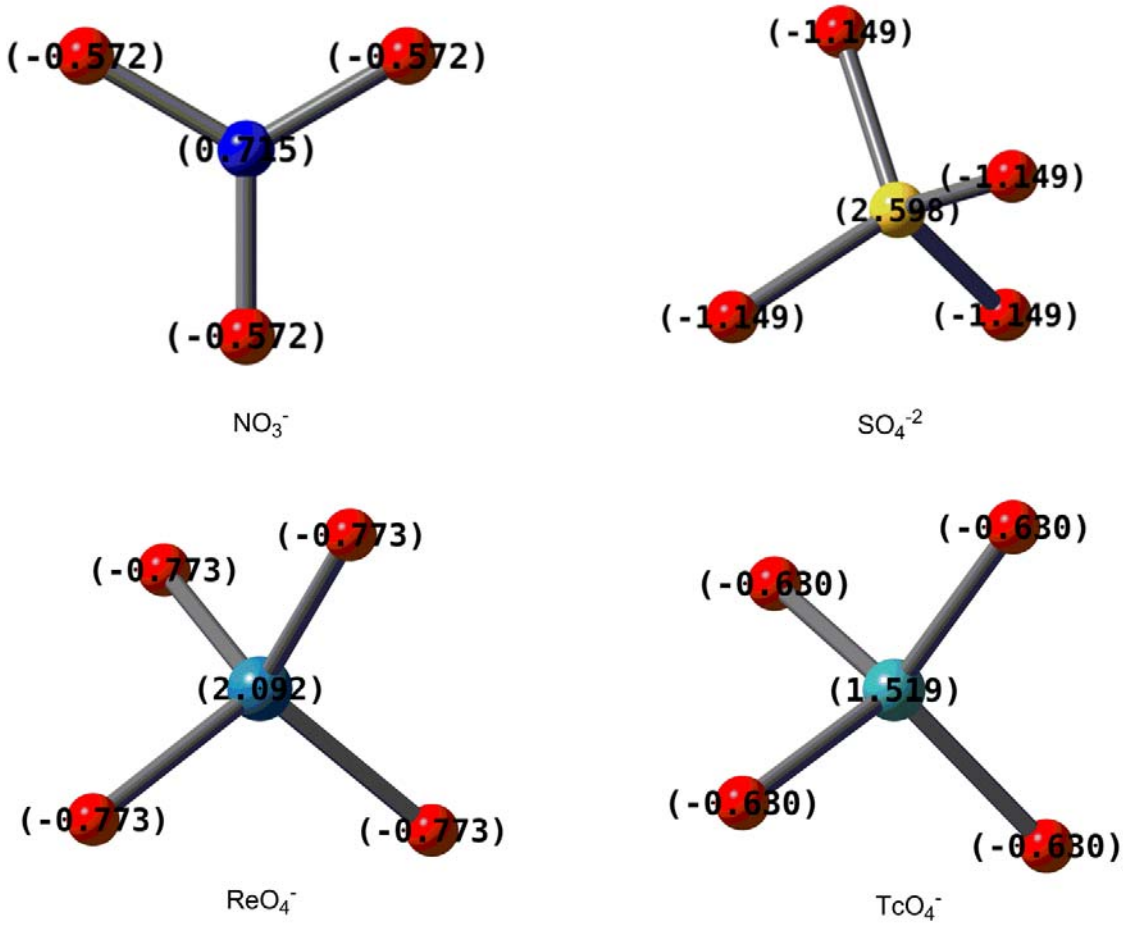

Figure S24. The charges of atoms in NO_3^-, SO_4^{2-}, ReO_4^- and TcO_4^- calculated via NBO analysis.

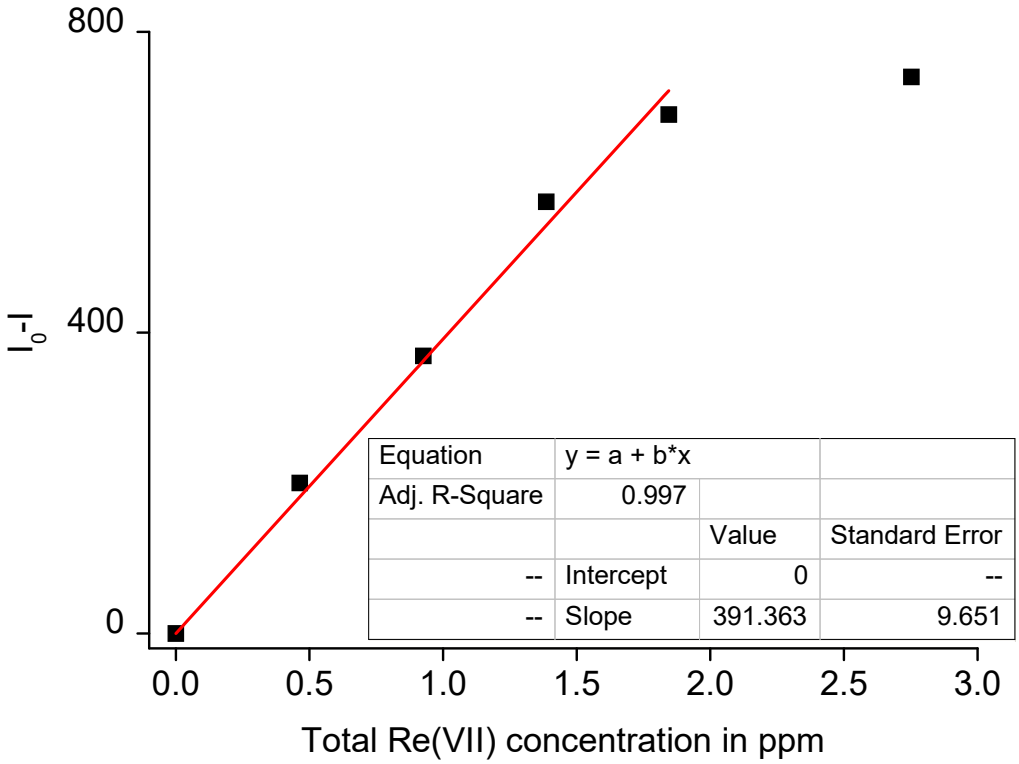

Figure S25. Calibration curve of the titration of an aqueous suspension of **MOR-2** (pH 5) with ReO_4^-.

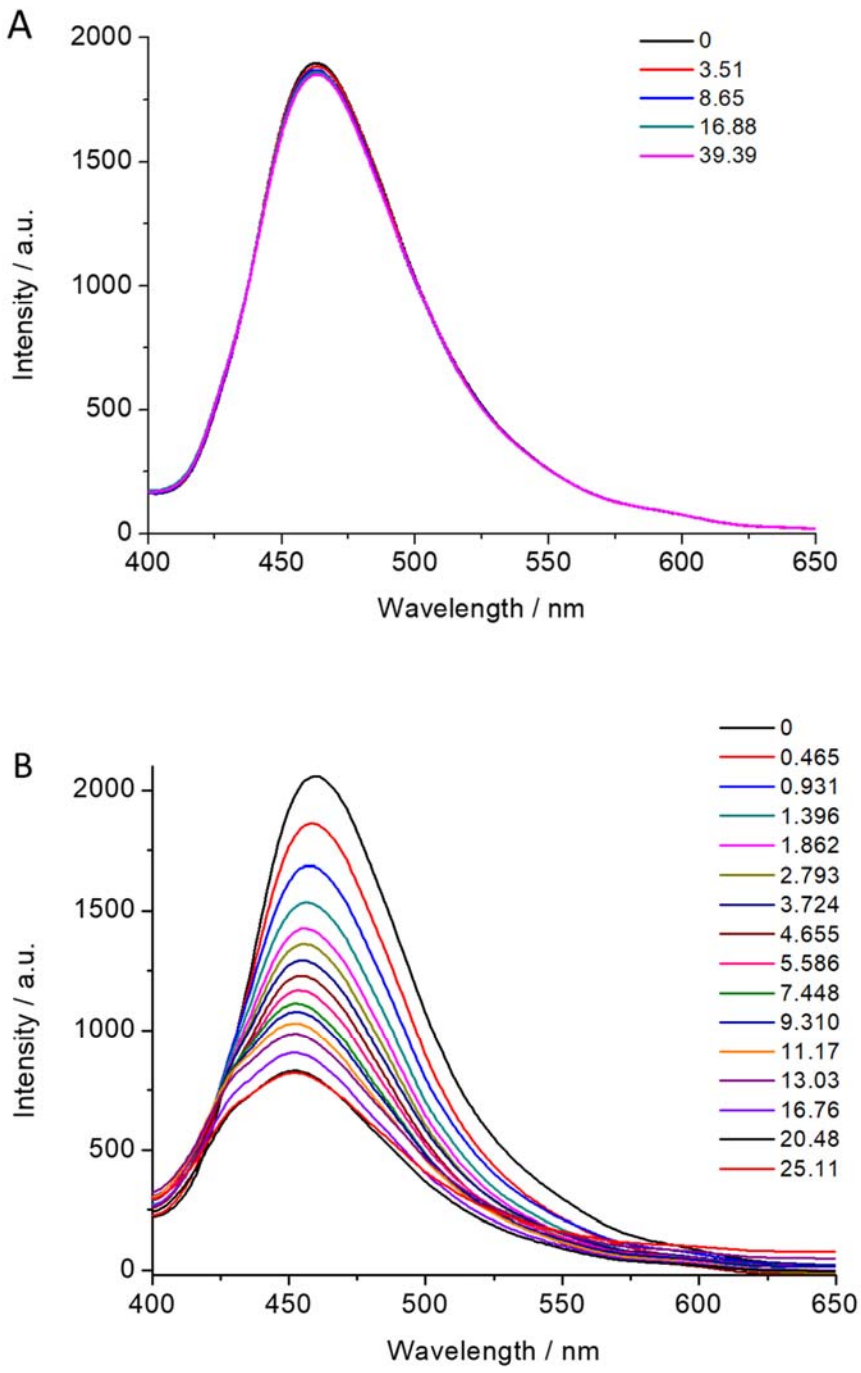
A
2000
1500
1000
500
0
Intensity / a.u.
400
450
500
550
600
650
Wavelength / nm
0
3.51
8.65
16.88
39.39
B
2000
1500
1000
500
0
Intensity / a.u.
400
450
500
550
600
650
Wavelength / nm
0
0.465
0.931
1.396
1.862
2.793
3.724
4.655
5.586
7.448
9.310
11.17
13.03
16.76
20.48
25.11

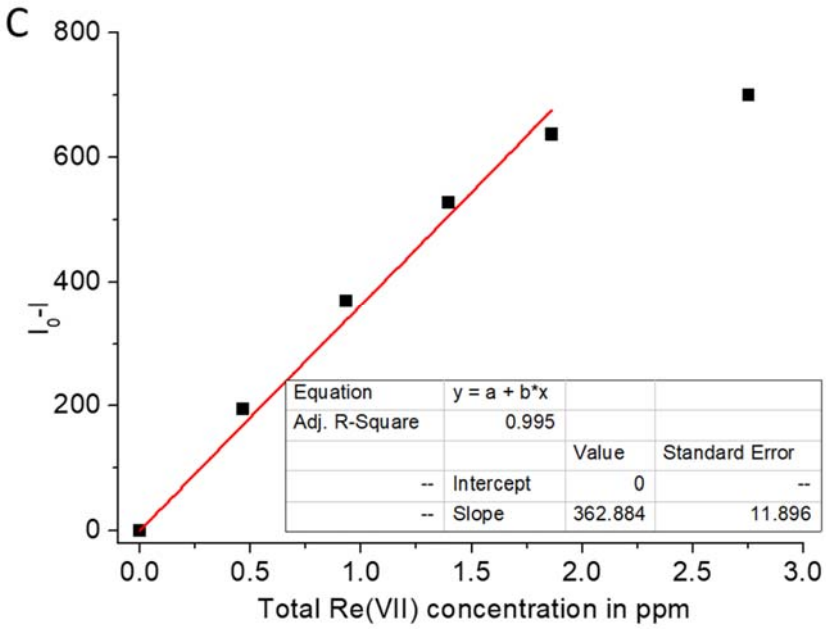

Figure S26. **A.** Blank experiment of an aqueous suspension of **MOR-2** (pH 5) with KCl, **B.** Titration of an aqueous suspension of **MOR-2** (pH 5) with ReO_4^- in the presence of a ten-fold excess of Cl^- anions, **C.** Calibration curve of the titration of an aqueous suspension of MOR-2 (pH 5) with ReO_4^- in the presence of a ten-fold excess of Cl^- anions (with respect to ReO_4^-).

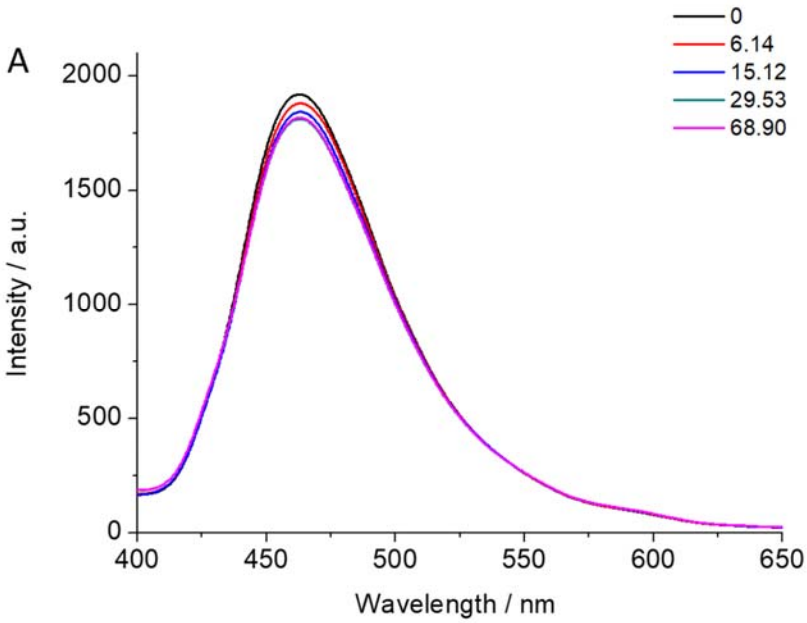
A
0
6.14
15.12
29.53
68.90
Intensity / a.u.
Wavelength / nm

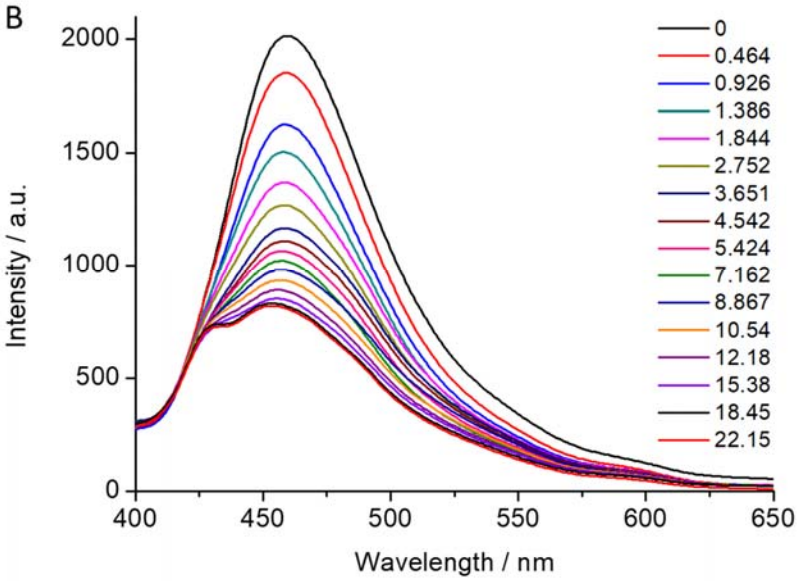
B
0
0.464
0.926
1.386
1.844
2.752
3.651
4.542
5.424
7.162
8.867
10.54
12.18
15.38
18.45
22.15
Intensity / a.u.
Wavelength / nm

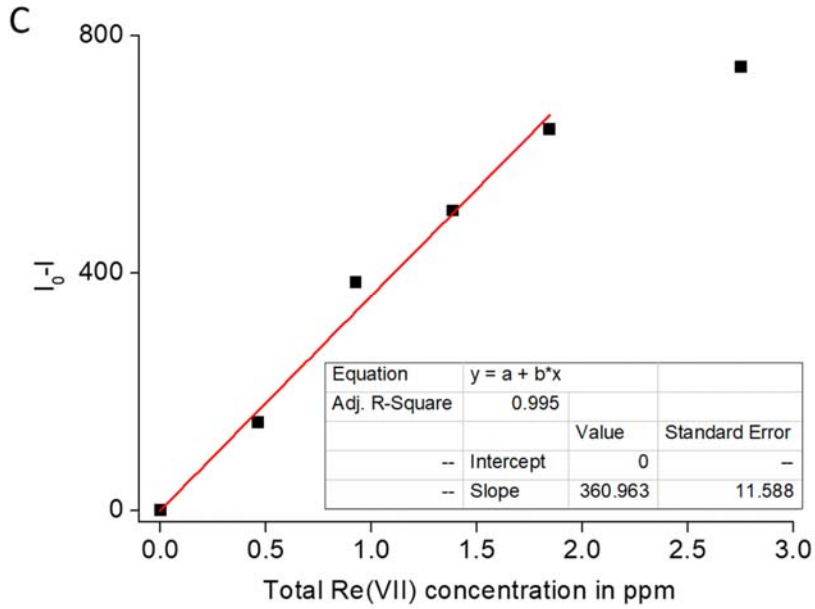

Figure S27. A. Blank experiment of an aqueous suspension of **MOR-2** (pH 5) with $NaNO_3$, **B.** Titration of an aqueous suspension of **MOR-2** (pH 5) with ReO_4^- in the presence of a ten-fold excess of NO_3^- anions, **C.** Calibration curve of the titration of an aqueous suspension of **MOR-2** (pH 5) with ReO_4^- in the presence of a ten-fold excess of NO_3^- anions (with respect to ReO_4^-).

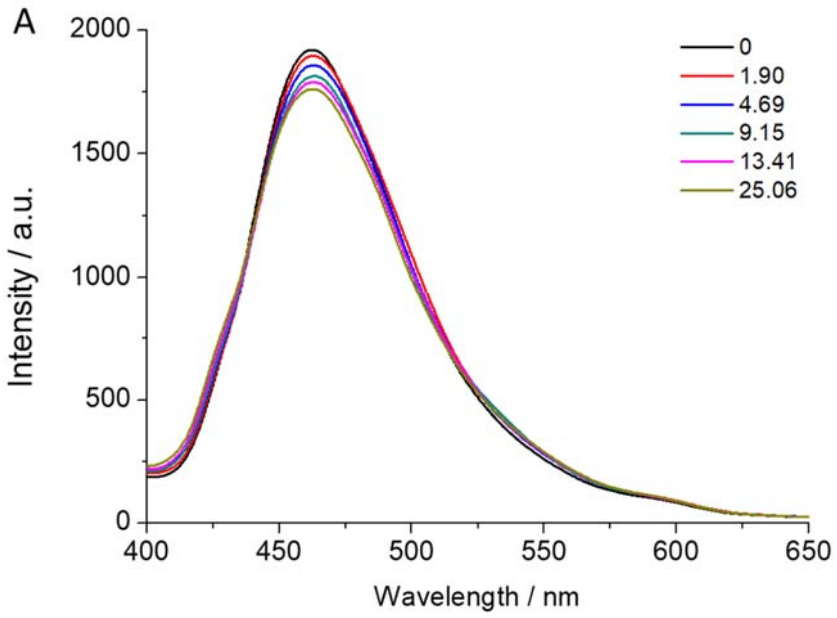
A
2000
1500
1000
500
0
Intensity / a.u.
400
450
500
550
600
650
Wavelength / nm
0
1.90
4.69
9.15
13.41
25.06

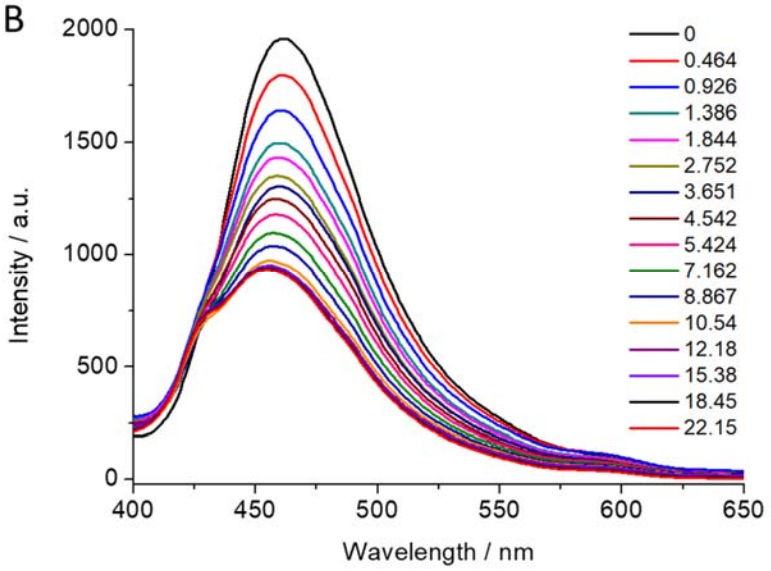
B
2000
1500
1000
500
0
Intensity / a.u.
400
450
500
550
600
650
Wavelength / nm
0
0.464
0.926
1.386
1.844
2.752
3.651
4.542
5.424
7.162
8.867
10.54
12.18
15.38
18.45
22.15

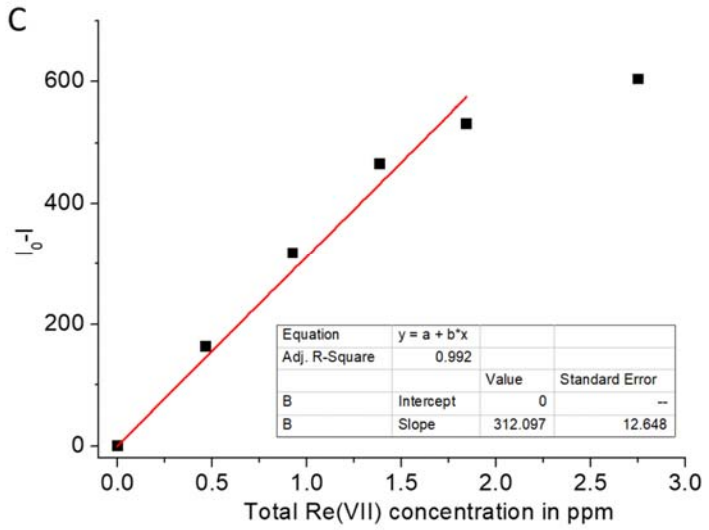

Figure S28. **A.** Blank experiment of an aqueous suspension of **MOR-2** (pH 5) with Na_2SO_4, **B.** Titration of an aqueous suspension of **MOR-2** (pH 5) with ReO_4^- in the presence of a two-fold excess of SO_4^- anions, **C.** Calibration curve of the titration of an aqueous suspension of **MOR-2** (pH 5) with ReO_4^- in the presence of a two-fold excess of SO_4^- anions (with respect to ReO_4^-).

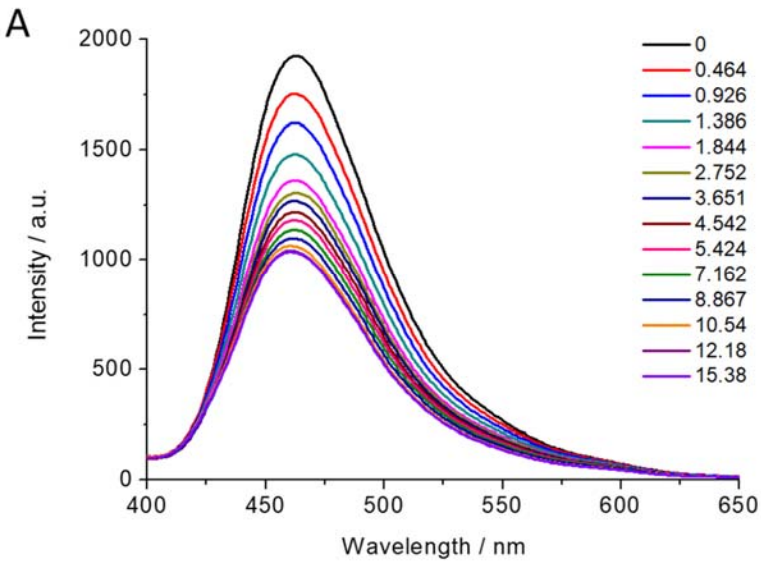

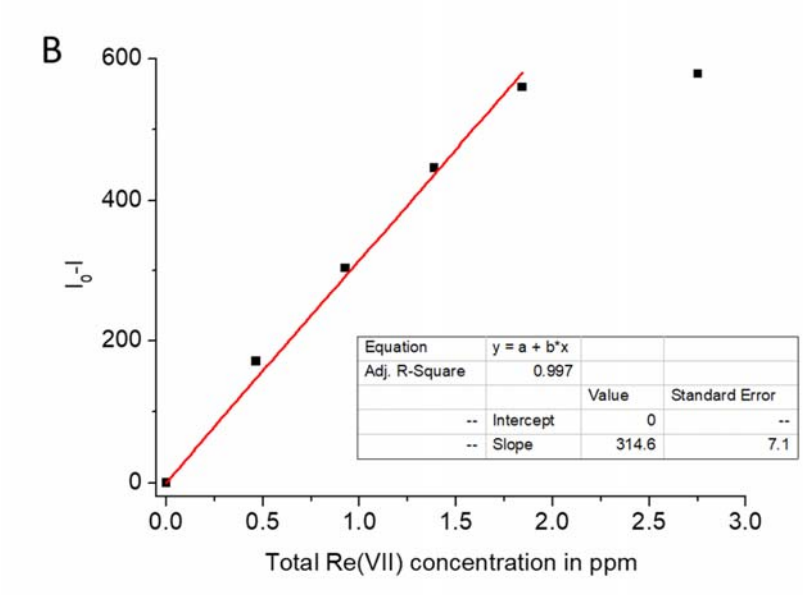

Figure S29. **A.** Titration of an aqueous suspension of **MOR-2** (pH 5) with ReO_4^- in potable water, **B.** Calibration curve of the titration of an aqueous suspension of **MOR-2** (pH 5) with ReO_4^- in potable water.

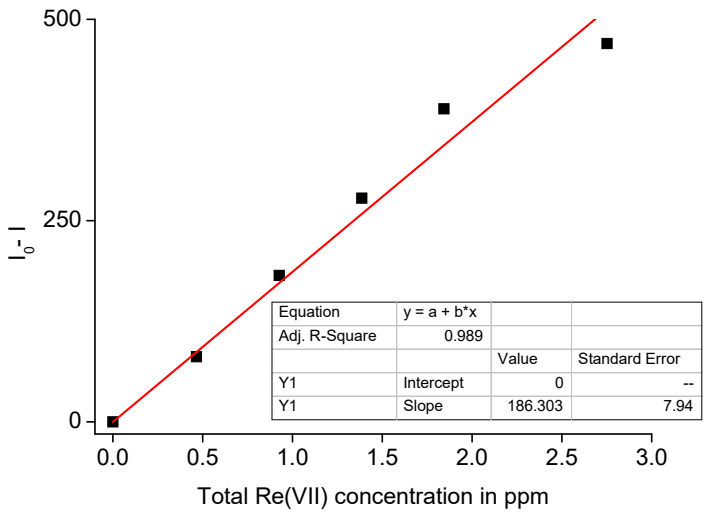

Figure S30. Calibration curve of the titration of an aqueous suspension of **MOR-1 (pH 5)** with ReO_4^-.

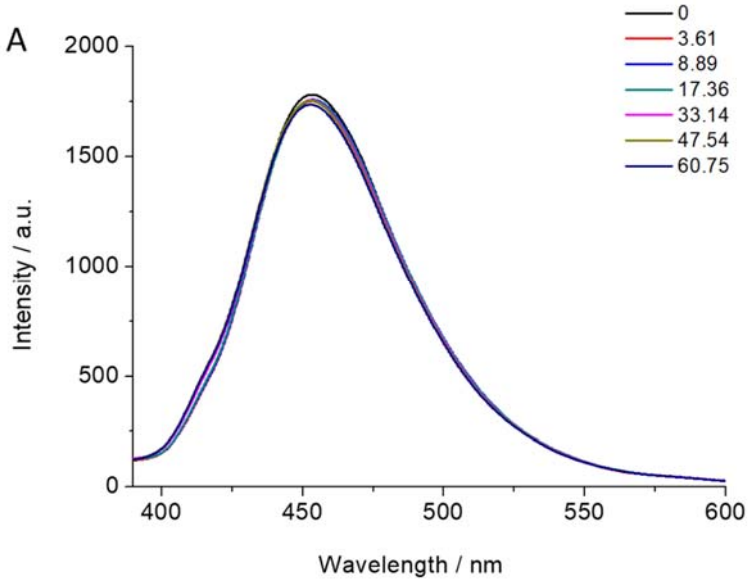
A
Intensity / a.u.
Wavelength / nm
0
3.61
8.89
17.36
33.14
47.54
60.75

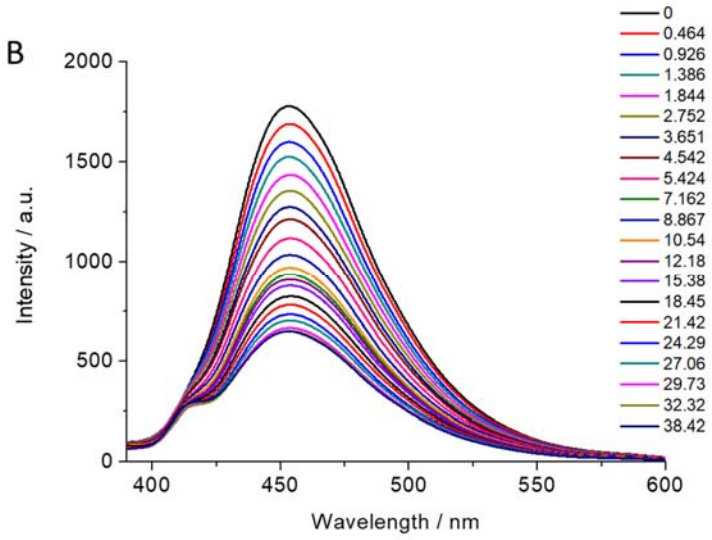
B
Intensity / a.u.
Wavelength / nm
0
0.464
0.926
1.386
1.844
2.752
3.651
4.542
5.424
7.162
8.867
10.54
12.18
15.38
18.45
21.42
24.29
27.06
29.73
32.32
38.42

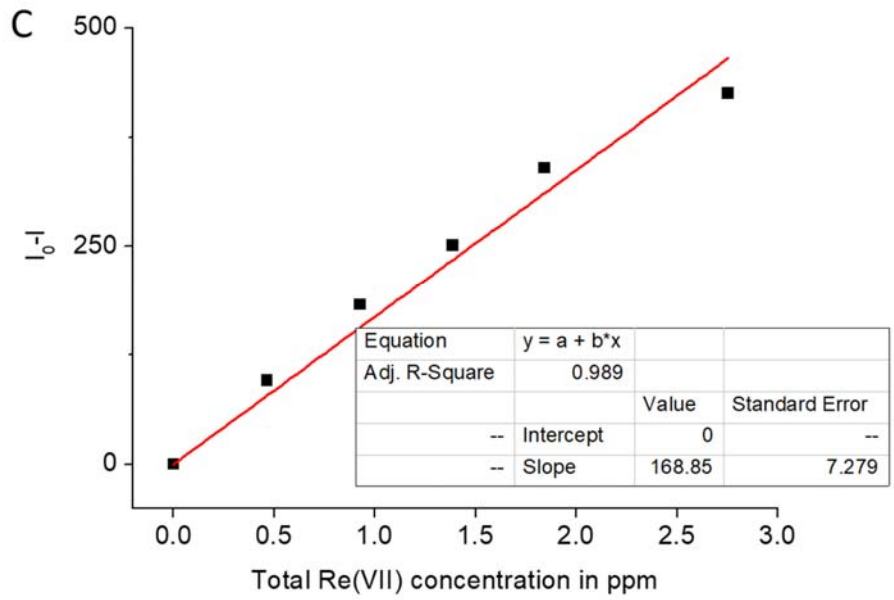

Figure S31. **A**. Blank experiment of an aqueous suspension of **MOR-1** (pH 5) with KCl, **B**. Titration of an aqueous suspension of **MOR-1** (pH 5) with ReO_4^- in the presence of a ten-fold excess of Cl- anions, **C**. Calibration curve of the titration of an aqueous suspension of **MOR-1** (pH 5) with ReO_4^- in the presence of a ten-fold excess of Cl^- anions (with respect to ReO_4^-).

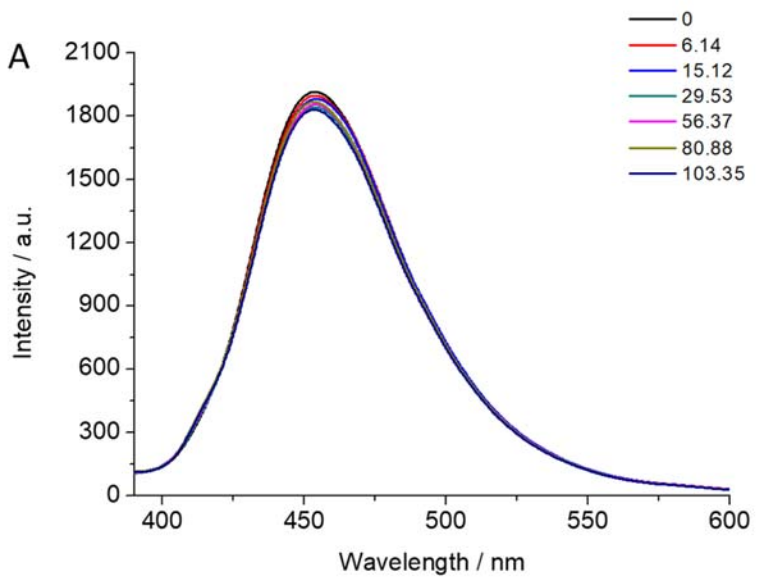

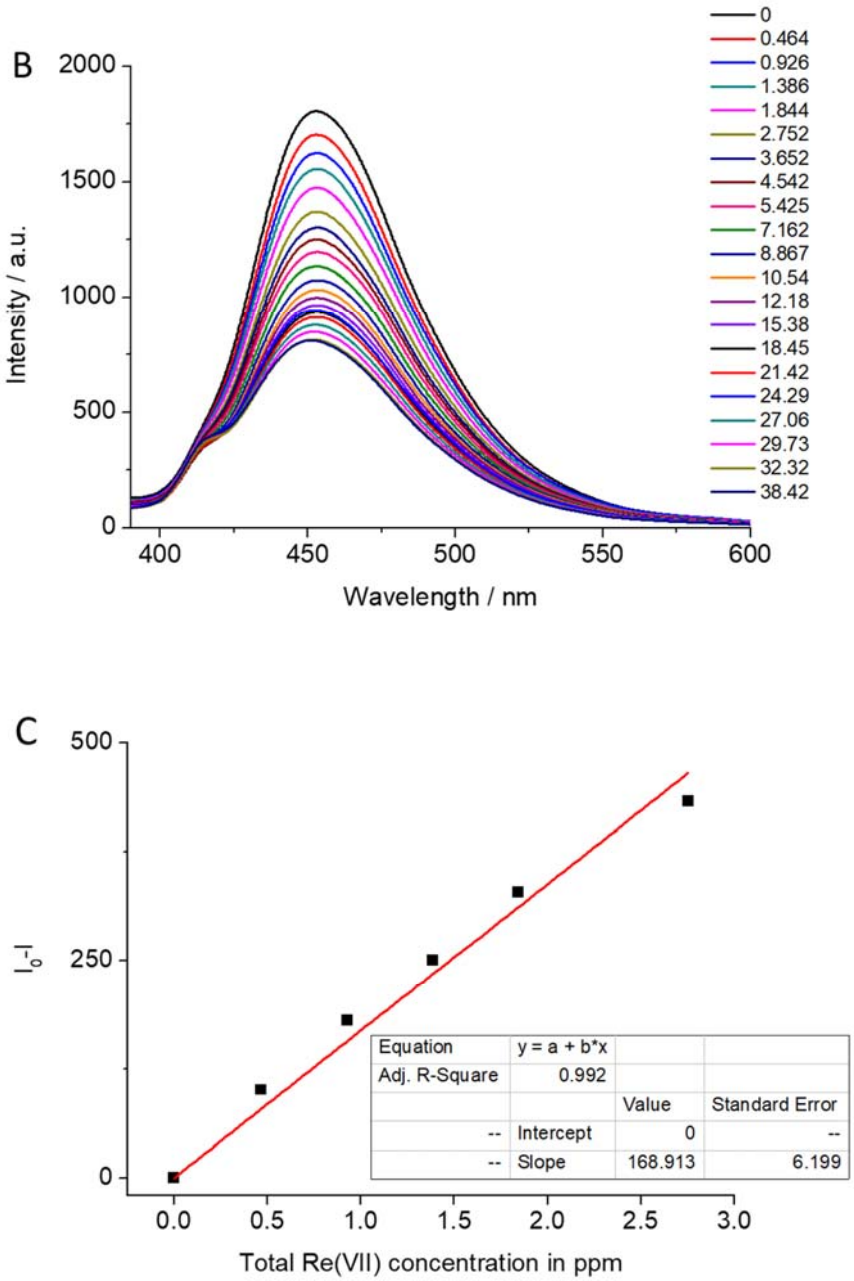

Figure S32. **A**. Blank experiment of an aqueous suspension of **MOR-1** (pH 5) with $NaNO_3$, **B**. Titration of an aqueous suspension of **MOR-1** (pH 5) with ReO_4^- in the presence of a ten-fold excess of NO_3^- anions, **C**. Calibration curve of the titration of an aqueous suspension of **MOR-1** (pH 5) with ReO_4^- in the presence of a ten-fold excess of NO_3^- anions (with respect to ReO_4^-).

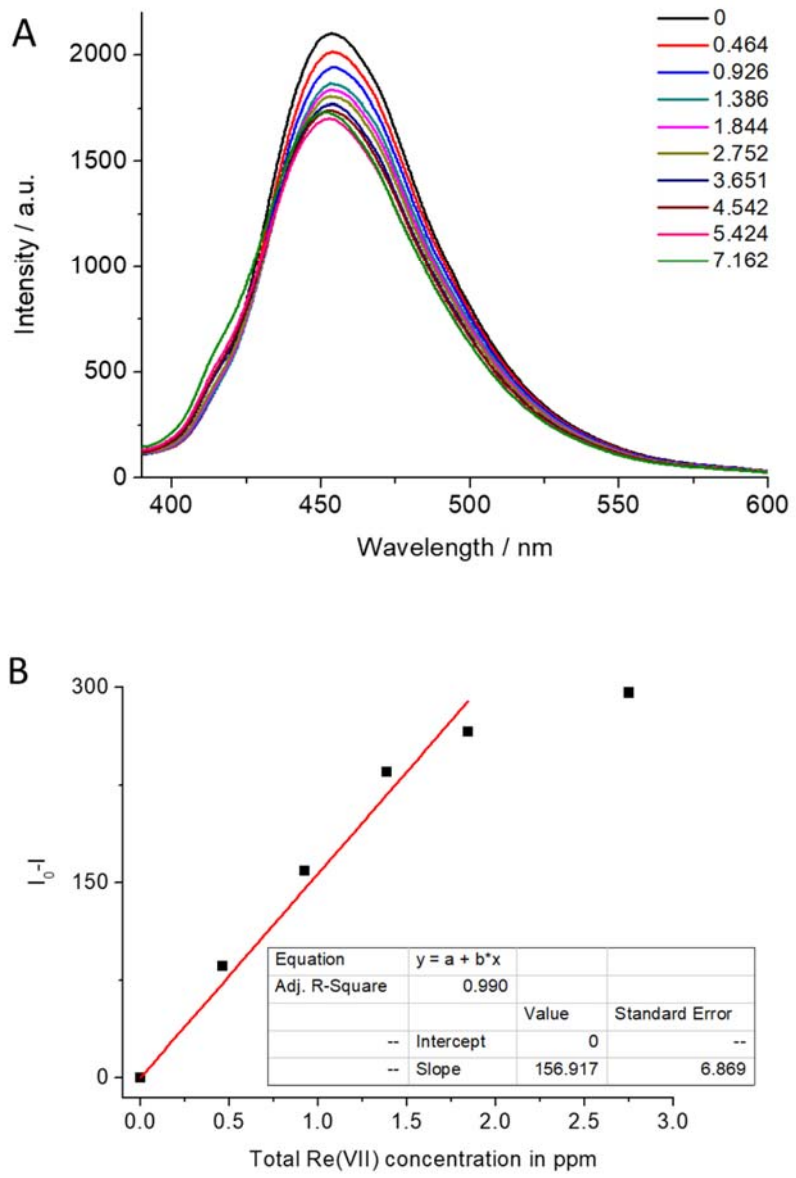

Figure S33. **A**. Titration of an aqueous suspension of **MOR-1** (pH 5) with ReO_4^- in the presence of a two-fold excess of SO_4^- anions, **C**. Calibration curve of the titration of an aqueous suspension of **MOR-1** (pH 5) with ReO_4^- in the presence of a two-fold excess of SO_4^- anions (with respect to ReO_4^-).

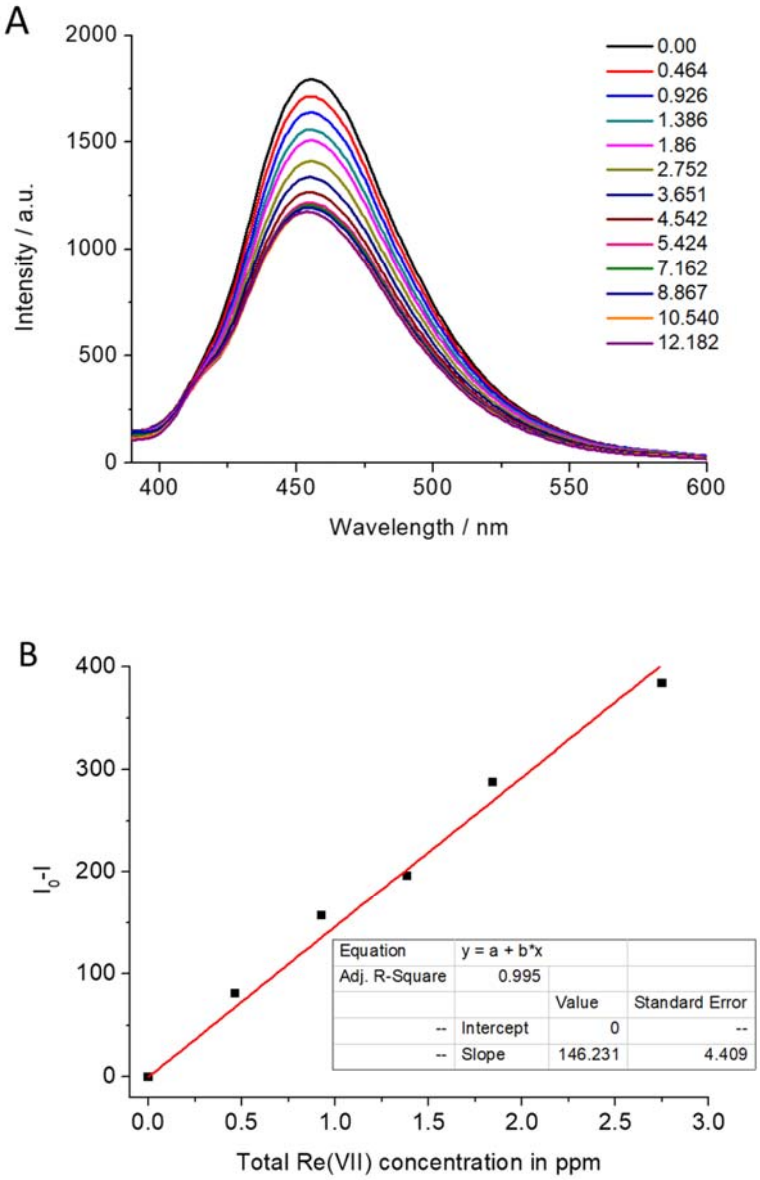

Figure S34. **A.** Titration of an aqueous suspension of **MOR-1** (pH 5) with ReO_4^- in potable water, **B.** Calibration curve of the titration of an aqueous suspension of **MOR-1** (pH 5) with ReO_4^- in potable water.

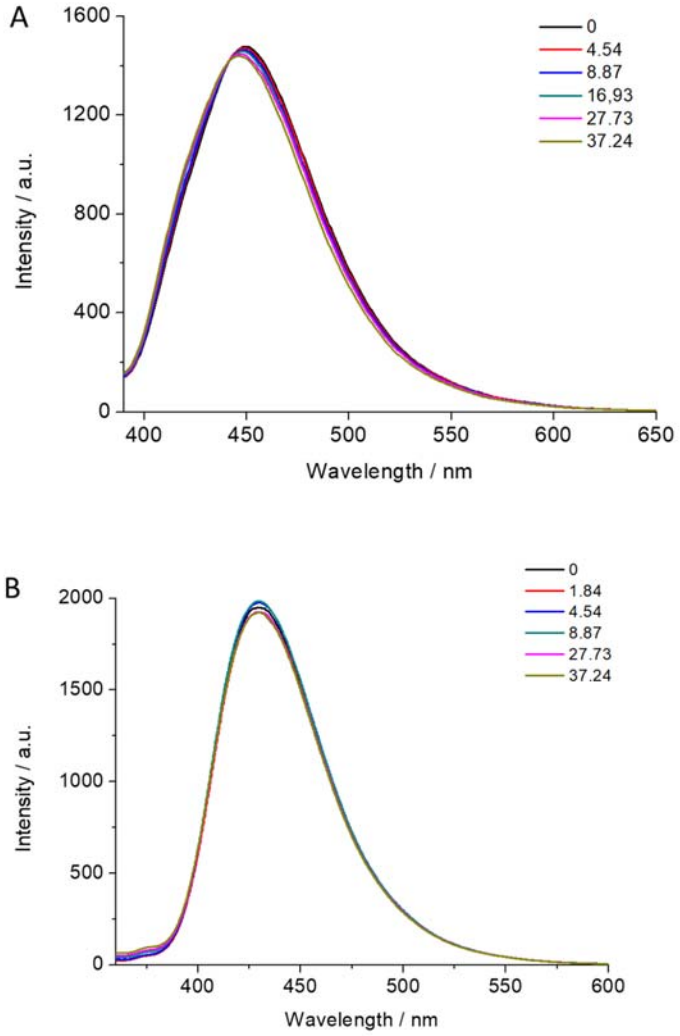

Figure S35. A. Titration of aqueous suspensions (pH 5) of deactivated samples of **MOR-2** (**A**) and **MOR-1** (**B**) with ReO_4^-. The samples were deactivated by stirring overnight in methanol in the presence of a ten-fold excess of triethylamine followed by excessive washing with methanol and water.

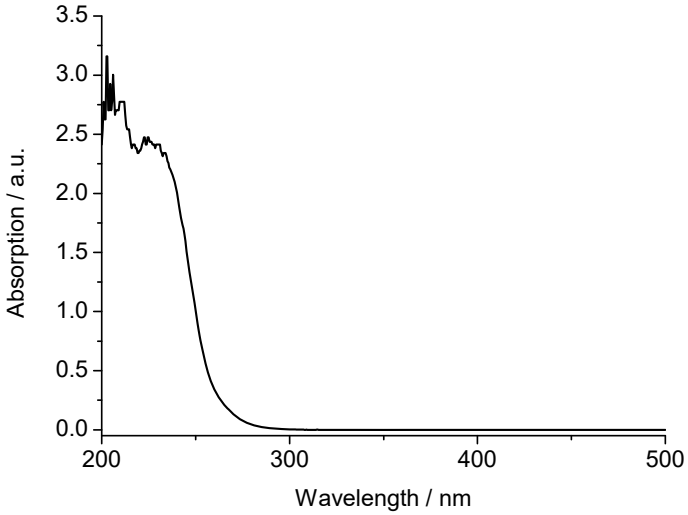

Figure S36. Absorption profile of NH_4ReO_4 (10^{-3} M) in water.